Dispersive techniques for lattice analysis

J. Ruiz de Elvira

Institute for Theoretical Physics, University of Bern

Multi-Hadron Systems from Lattice QCD, Seattle, February 6th, 2018

Outline

Why are dispersive techniques useful for Lattice QCD?

Dispersion relations: advantages and limitations

↪ Roy and Roy-Steiner equations

Dispersive techniques in meson-meson scattering

↪ Roy equation analysis for pion-pion scattering

in collaboration with R. G. Martin, R. Kaminski, J.R. Pelaez

Dispersive techniques in meson-nucleon scattering

↪ Roy-Steiner equation analysis for pion-nucleon scattering

in collaboration with M. Hoferichter, B. Kubis and U-G. Meißner

Prospects of dispersive techniques for lattice analyses

↪ Roy equation for unphysical pion masses

in collaboration with G. Colangelo

Dispersion relations in a nutshell

- Effective field theories $\Rightarrow$ systematically improvable but
  - ▷ number of LECs increase rapidly
  - ▷ **convergence** problems: low-lying resonances, strong rescattering effects
- Dispersion relations: **analyticity**, **crossing**, **unitarity**
  - ▷ analitycity constrains the energy depedence of scattering amplitude
  - ▷ crossing symmetry connects different physical regions
  - ▷ unitarity constrains imaginary part
- **Roy(-Steiner) eqs.** =Partial-Wave (Hyberbolic) Dispersion Relations coupled by unitarity and crossing symmetry
  - $\hookrightarrow$ **model independent** aproach
  - $\hookrightarrow$ **analytic continuation** for the complex plane $\Rightarrow$ resonances, unphysical regions

From Cauchy's theorem to dispersion relations

- Cauchy's Theorem

$$f(s) = \frac{1}{2\pi i}\int_{\partial\Omega} \frac{ds' f(s')}{s' - s}$$

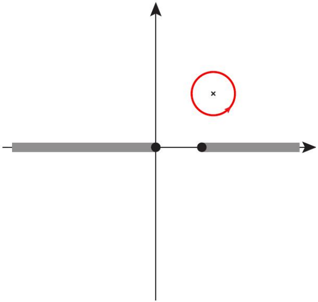

From Cauchy's theorem to dispersion relations

- Cauchy's Theorem

$$f(s) = \frac{1}{2\pi i}\int_{\partial\Omega} \frac{ds' f(s')}{s' - s}$$

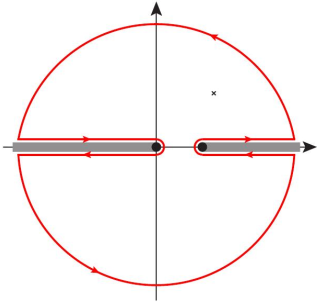

From Cauchy's theorem to dispersion relations

- Dispersion relation

$$f(s) = \frac{1}{\pi}\int_{\text{cuts}} \frac{ds'\,\text{Im}\, f(s')}{s'-s}$$

$\hookrightarrow$ **analyticity**

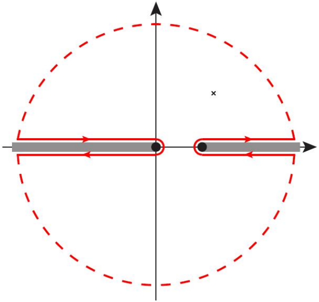

From Cauchy's theorem to dispersion relations

- Dispersion relation

$$f(s) = \frac{1}{\pi}\int_{\text{cuts}} \frac{ds'\,\mathrm{Im}\,f(s')}{s'-s}$$

$\hookrightarrow$ **analyticity**

- Subtractions

$$f(s) = f(0) + \frac{s}{\pi}\int_{\text{cuts}} \frac{ds'\,\mathrm{Im}\,f(s')}{s'(s'-s)}$$

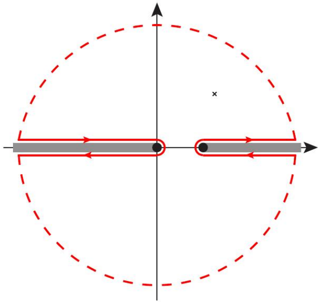

From Cauchy's theorem to dispersion relations

- Dispersion relation

$$f(s) = \frac{1}{\pi}\int_{\text{cuts}} \frac{ds' \, \mathrm{Im}\, f(s')}{s'-s}$$

$\hookrightarrow$ **analyticity**

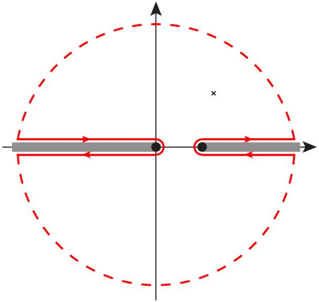

- Subtractions

$$f(s) = f(0) + \frac{s}{\pi}\int_{\text{cuts}} \frac{ds' \, \mathrm{Im}\, f(s')}{s'(s'-s)}$$

- Imaginary part from **Cutkosky rules**
  $\hookrightarrow$ forward direction: optical theorem

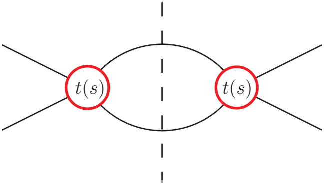

- Unitarity for partial waves

$$\mathrm{Im}\, f(s) = \sigma(s)|f(s)|^2, \quad f(s) = \frac{\eta(s)e^{2i\delta_{IJ}(s)}-1}{2i\sigma(s)}, \quad \sigma(s) = \sqrt{1-\frac{4m_\pi^2}{s}}$$

From dispersion relations to Roy-equations

- $\pi\pi \to \pi\pi \Rightarrow$ fully crossing symmetric in Mandelstam variables s, t, and $u = 4M_\pi - s - t$
- Start from twice-subtracted **fixed-t** DRs

$$T^I(s,t) = c(t) + \frac{1}{\pi}\int_{4m_\pi^2}^{\infty} \frac{ds'}{s'^2}\left[\frac{s^2}{(s'-s)} - \frac{u^2}{(s'-u)}\right]\mathrm{Im}\,T^I(s',t)$$

- Subtraction functions c(t) are determined via crossing symmetry

  $\hookrightarrow$ functions of the I=0,2 scattering lengths: a_0^0 and a_0^2

- PW-projection and expansion yields the **Roy-equations** [Roy (1971)]

$$t_J^I(s) = ST_J^I(s) + \sum_{J'=0}^{\infty}(2J'+1)\sum_{I'=0,1,2}\int_{4m_\pi^2}^{\infty} ds' K_{JJ'}^{II'}(s',s)\,\mathrm{Im}\,t_{J'}^{I'}(s')$$

- $K_{JJ'}^{II'}(s',s) \equiv$ kernels $\Rightarrow$ analytically known

Roy equations: range of convergence

- Convergence for $T^I(s,t)$ guaranteed for $t < 4m^2$
- Where does the partial wave expansion converge?
- Assumption: Mandelstam analyticity [Mandelstam (1958,1959)]

$$T(s,t) = \frac{1}{\pi^2}\iint ds'dt' \frac{\rho_{st}(s',t')}{(s'-s)(t'-t)} + (t \leftrightarrow u) + (s \leftrightarrow u)$$

$\hookrightarrow$ integration on the support of the double spectral densities ρ

- Boundaries of ρ

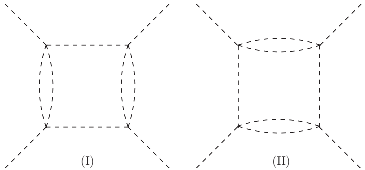

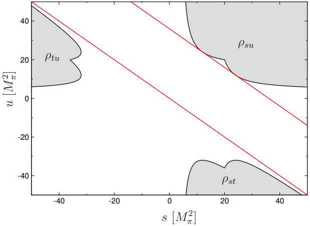

- Lehmann ellipses

$\hookrightarrow$ largest ellipses, which do not enter any ρ [Lehmann (1958)]

Solving Roy-equations: flow information

- **Roy-equations** rigorously valid for a finite energy range

  $\Rightarrow$ introduce a matching point s_m

- only partial waves with $J \leq J_{\max}$ are solved
- Assume **isospin limit**
- **Input**
  - High-energy region: $\mathrm{Im}\,t_J^I(s)$ for $s \geq s_m$ and for all J
  - Higher partial waves: $\mathrm{Im}\,t_J^I(s)$ for $J > J_{\max}$ and for all s
  - Inelasticities $\eta(s)$
- **Output**
  - Self-consistent solution for $\delta_{IJ}(s)$ for $J \leq J_{\max}$ and $s_{\mathrm{th}} \leq s \leq s_m$
  - Subtraction constants

Roy-equations: existence and uniqueness

- Solution characterized by subtraction constants and high-energy input (a, A)
- **Existence** and **uniqueness** depends on δ_i dynamically at s_m

$$m = \sum_i m_i, \qquad m_i = \begin{cases} \left\lfloor \frac{2\delta_i(s_\text{m})}{\pi} \right\rfloor & \text{if } \delta_i(s_\text{m}) > 0, \\ -1 & \text{if } \delta_i(s_\text{m}) < 0, \end{cases}$$

$$\lfloor x \rfloor \Rightarrow \text{largest integer} \leq x.$$

[Gasser, Wanders 1999, Wanders 2000]

- $m = 0$, a unique solution exists for any (a, A)
- $m > 0$, m-parameter family of solutions for any (a, A)
- $m < 0$, only for a specific choice of the input constrained by $|m|$ conditions
- **Physical solution** characterized by *smooth* matching

Roy-equations: $\pi\pi$ results

Solution for the $\pi\pi$ S0-wave

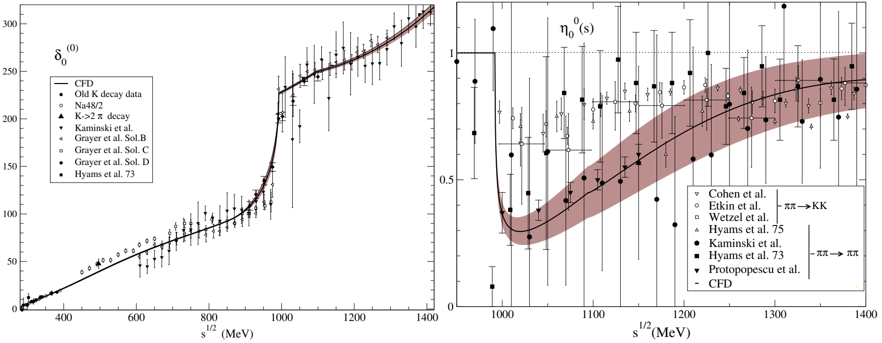

Garcia-Martin, Kaminski, Pelaez, JRE (2011)

Dip vs no-dip solutions

- The dip vs no-dip ⇒ long-standing controversy [Pennington, Bugg, Zou, Achasov] · · ·
  ↪ no clear preference for any of the two scenarios in previous works
- Is it possible to satisfy Roy Equations with a non-dip scenario?

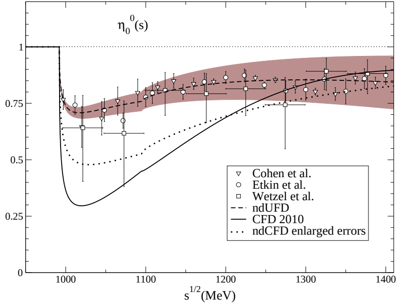

↪ the non-dip scenario is **rejected** by DR

- $t_{IJ}(s)$ known in the Lehmann ellipsis
- **Resonances**

  $\hookrightarrow$ poles on unphysical Riemann sheets
- $S^{II}(s - i\epsilon, t) = S^{I}(s + i\epsilon, t)$

  $\hookrightarrow$ $t^{II}_{IJ}(s) = t_{IJ}(s) \cdot (\mathbb{1} + 2i\,\Sigma(s) t_{IJ}(s))^{-1}$
- Elastic scattering: **II** RS is **known** exactly
- Coupled channels

$$t_{IJ}(s) = \begin{pmatrix} t^{(11)}_{IJ}(s) & t^{(12)}_{IJ}(s) \\ t^{(12)}_{IJ}(s) & t^{(22)}_{IJ}(s) \end{pmatrix}$$

$$\Sigma(s) = \begin{pmatrix} \sigma_1(s) & 0 \\ 0 & \sigma_2(s) \end{pmatrix}$$

$\hookrightarrow$ III and IV RS require crossed channels

$$t^{IV}_{IJ}(s) = t^{(11)}_{IJ}(s) - \frac{2i\sigma_2(s) t^{(12)}_{IJ}(s)^2}{1 + 2i\sigma_2(s) t^{(22)}_{IJ}(s)}$$

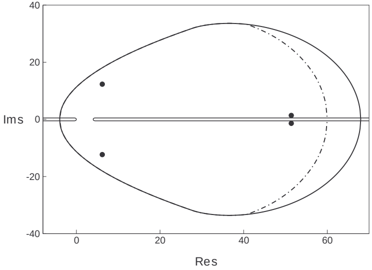

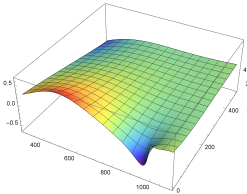

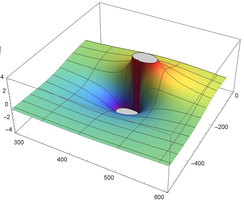

$f_0(500)$ pole 2010

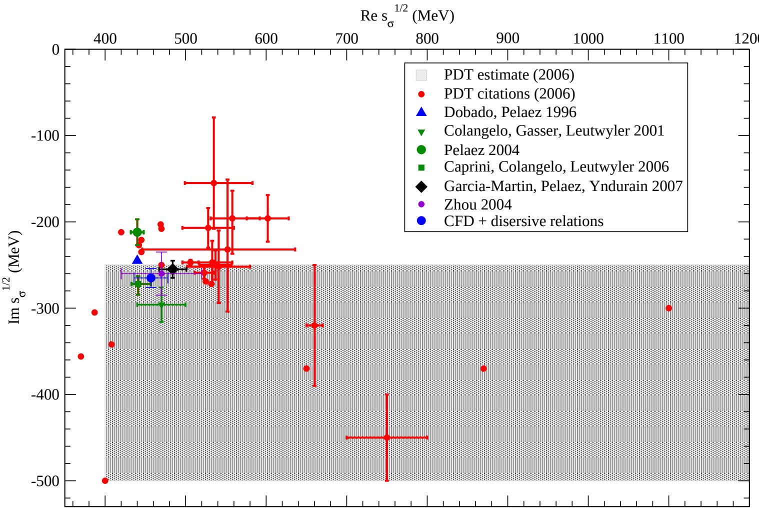

$f_0(500)$ pole 2012

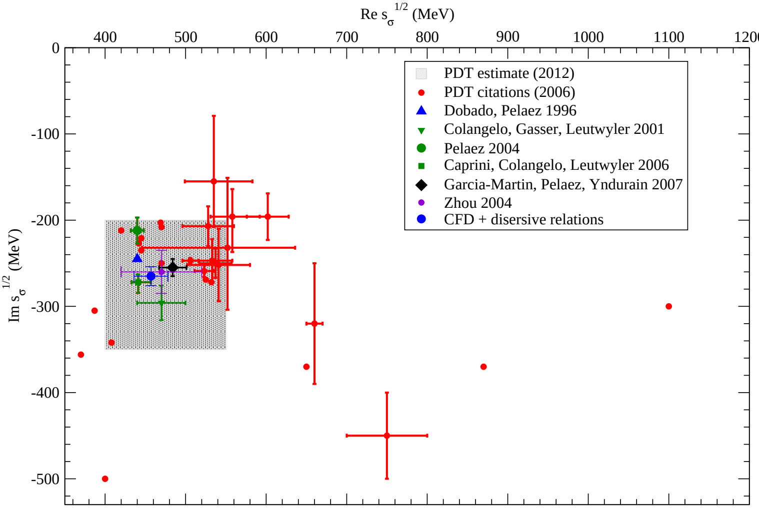

$f_0(980)$ pole 2010

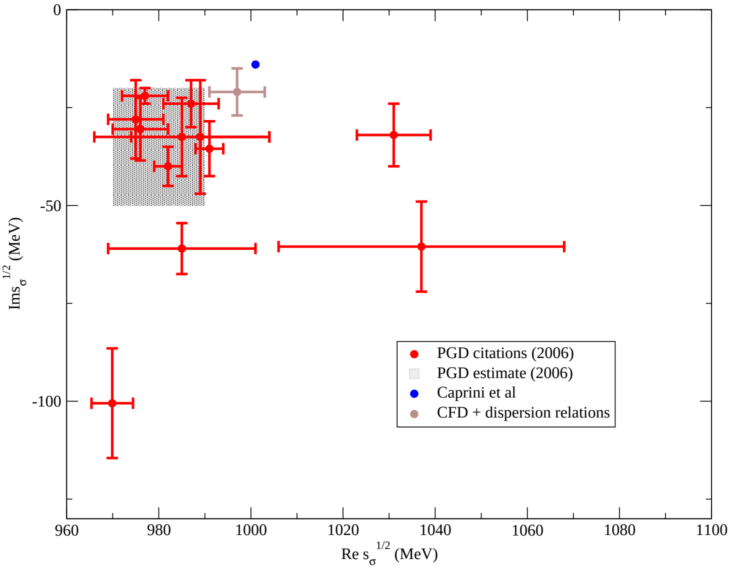

$f_0(980)$ pole 2012

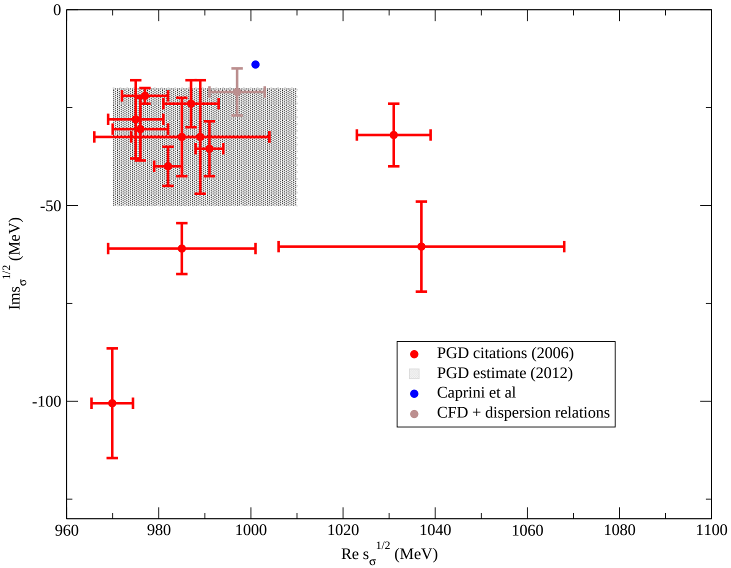

Roy–Steiner equations for πN: differences to $\pi\pi$ Roy equations

Key differences compared to $\pi\pi$ Roy equations

- Crossing: coupling between $\pi N \to \pi N$ (s-channel) and $\pi\pi \to \bar{N}N$ (t -channel)

  $\Rightarrow$ need a different kind of dispersion relations [Hite, Steiner 1973, Büttiker et al. 2004]

- Unitarity in t-channel, e.g. in single-channel approximation

$$\mathrm{Im} f_{\pm}^{J}(t) = \sigma_t^{\pi} f_{\pm}^{J}(t) t_J^{I}(t)^*$$

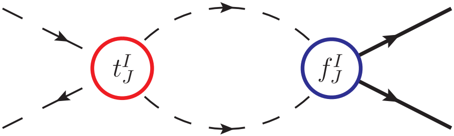

  $\Rightarrow$ **Watson's theorem**: phase of $f_{\pm}^{J}(t)$ equals δ_{IJ} [Watson 1954]

  $\hookrightarrow$ solution in terms of Omnès function [Muskhelishvili 1953, Omnès 1958]

- Large pseudo-physical region in t -channel

  $\hookrightarrow$ $\bar{K}K$ intermediate states for s-wave in the region of the $f_0(980)$

Roy–Steiner equations for πN: flow of information

Limited range of validity

$$\sqrt{s} \leq \sqrt{s_m} = 1.38\,\mathrm{GeV} \qquad \sqrt{t} \leq \sqrt{t_m} = 2.00\,\mathrm{GeV}$$

Input/Constraints

- S- and P-waves above matching point $s > s_m$ $(t > t_m)$
- Inelasticities
- Higher waves (D-, F-, $\cdots$)
- Scattering lengths from hadronic atoms

[Baru et al. 2011]

Output

- S- and P-wave phase-shifts at low energies $s < s_m$ $(t < t_m)$
- Subthreshold parameters
  - ▷ Pion-nucleon σ-term
  - ▷ Nucleon form factor spectral functions
  - ▷ ChPT LECs

Results: s-channel pw

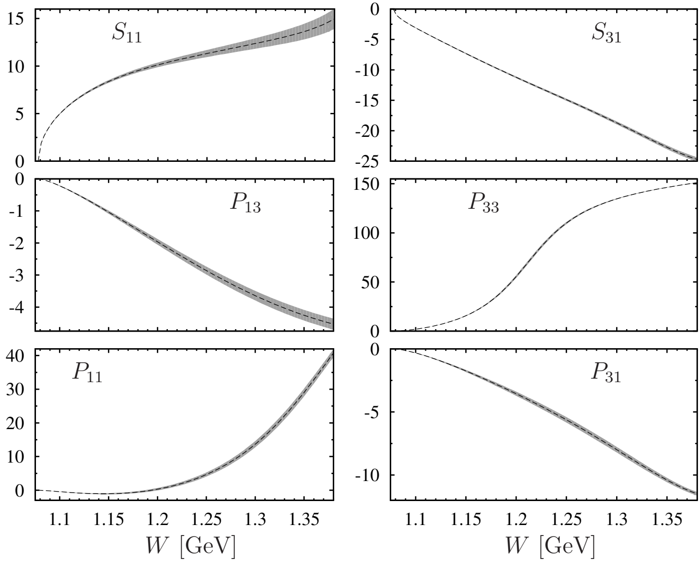

Results: t-channel pw

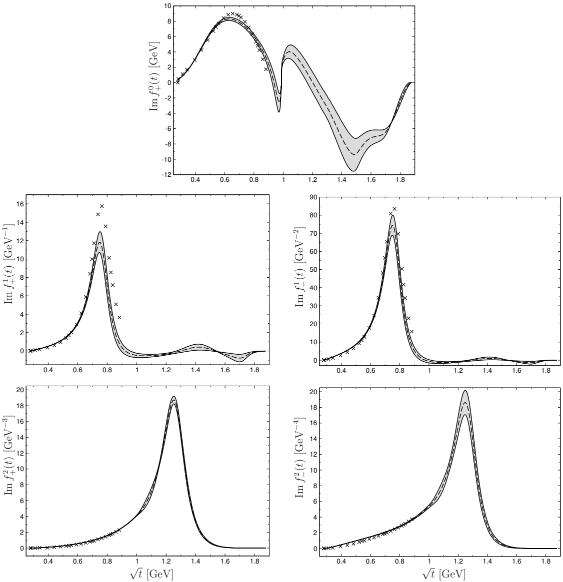

Threshold parameters

- Threshold parameters defined as: $\text{Re}\, f^I_{l\pm}(s) = q^{2l}\{a^I_{l\pm} + b^I_{l\pm} q^2 + \cdots\}$
- Extracted from hyperbolic sum rules:

$$a^{1/2}_{0+} = d^+_{00} + \frac{g^2}{m_N} + \frac{1}{\pi}\int_{t_\pi}^{\infty} \frac{dt'}{t'} \left\{ \left[\text{Im}\, A^+\right]_{(M_\pi,0)} - \left[\text{Im}\, A^+\right]_{(0,0)} \right\} + \frac{1}{\pi}\int_{s_+}^{\infty} ds' \left\{ h_+(s') \left[\text{Im}\, A^+\right]_{(M_\pi,0)} - (h_0(s')) \left[\text{Im}\, A^+\right]_{(0,0)} \right\},$$

	RS	KH80
$a^{1/2}_{0+}$ $[10^{-3} M_\pi^{-1}]$	169.8 ± 2.0	173 ± 3
$a^{3/2}_{0+}$ $[10^{-3} M_\pi^{-1}]$	-86.3 ± 1.8	-101 ± 4
$a^{1/2}_{1+}$ $[10^{-3} M_\pi^{-3}]$	-29.4 ± 1.0	-30 ± 2
$a^{3/2}_{1+}$ $[10^{-3} M_\pi^{-3}]$	211.5 ± 2.8	214 ± 2
$a^{1/2}_{1-}$ $[10^{-3} M_\pi^{-3}]$	-70.7 ± 4.1	-81 ± 2
$a^{3/2}_{1-}$ $[10^{-3} M_\pi^{-3}]$	-41.0 ± 1.1	-45 ± 2
$b^{1/2}_{0+}$ $[10^{-3} M_\pi^{-3}]$	-35.2 ± 2.2	-18 ± 12
$b^{3/2}_{0+}$ $[10^{-3} M_\pi^{-3}]$	-49.8 ± 1.1	-58 ± 9

- Disagreement in the $a^{3/2}_0$ scattering length in $\sim 4\sigma$

The pion-nucleon σ-term

Scalar form factor of the nucleon:

$\sigma(t) = \langle N(p')|\hat{m}\,(\bar{u}u + \bar{d}d)\,|N(p)\rangle \qquad t = (p' - p)^2 \qquad \sigma_{\pi N} = \sigma(0)$

- $\sigma_{\pi N}$ measures the **light-quark contribution** to the nucleon mass
- Unfortunately, no direct experimental access to it
- Only very recent precise lattice results
- Linked to πN via the **Cheng-Dashen** theorem

[Cheng, Dashen 1971]

$$\underbrace{F_\pi^2 \bar{D}^+(\nu = 0, t = 2M_\pi^2)}_{F_\pi^2(d_{00}^+ + 2M_\pi^2 d_{01}^+) + \Delta_D} = \underbrace{\sigma(2M_\pi^2)}_{\sigma_{\pi N} + \Delta_\sigma} + \Delta_R$$

$|\Delta_R| \lesssim 2$ MeV [Bernard, Kaiser, Meißner 1996]

$\Delta_D - \Delta_\sigma = (-1.8 \pm 0.2)$ MeV [Hoferichter et al. 2012]

- "Canonical value" $\sigma_{\pi N} \sim 45$ MeV, based on KH80

[Gasser, Leutwyler, Locher, Sainio 1988,1991]

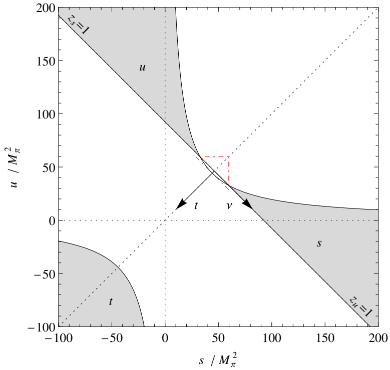

Results for the sigma-term

$$\sigma_{\pi N} = F_\pi^2 \left(d_{00}^+ + 2M_\pi^2 d_{01}^+ \right) + \Delta_D - \Delta_\sigma - \Delta_R$$

- subthreshold parameters output of the Roy–Steiner equations

  $d_{00}^+ = -1.36(3) M_\pi^{-1}$ [KH: $-1.46(10) M_\pi^{-1}$], $d_{01}^+ = 1.16(2) M_\pi^{-3}$ [KH: $1.14(2) M_\pi^{-3}$]

- $\Delta_D - \Delta_\sigma = -(1.8 \pm 0.2)\ \mathrm{MeV}$ [Hoferichter et al. 2012]

  $|\Delta_R| \lesssim 2$ MeV [Bernard, Kaiser, Meißner 1996]

- Isospin breaking in the CD theorem shifts $\sigma_{\pi N}$ by $+3.0$ MeV
- Final results: $\sigma_{\pi N} = (59.1 \pm 1.9_{\mathrm{RS}} \pm 3.0_{\mathrm{LET}})$ MeV=(59.1 ± 3.5) MeV [MH, JRE, Kubis, Meißner]
- $\sigma_{\pi N}$ depends linearly on the scattering lengths: $\sigma_{\pi N} = 59.1 + \sum_{I_s} c_{I_s} \Delta a_{0+}^{I_s}$
- KH input $\Rightarrow \sigma_{\pi N} = 46$ MeV

  $\hookrightarrow$ to be compared with $\sigma_{\pi N} = 45$ MeV [Gasser, Leutwyler, Socher, Sainio 1988]

Comparison with lattice $\sigma_{\pi N}$ results

- Recent lattice determination of $\sigma_{\pi N}$ at (almost) the physical point
  - ▷ BMW $\sigma_{\pi N} = 38(3)(3)$MeV [Durr et al. 2015]
  - ▷ χQCD $\sigma_{\pi N} = 44.4(7.4)(2.8)$MeV [Yang et al. 2015]
  - ▷ ETMC $\sigma_{\pi N} = 37.2(2.6)(4.7)$MeV [Abdel-Rehim et al. 2015]
  - ▷ RQCD $\sigma_{\pi N} = 35(6)$MeV [Bali et al. 2016]

- The linear dependence of $\sigma_{\pi N}$ on the scattering lengths introduces an additional constraint

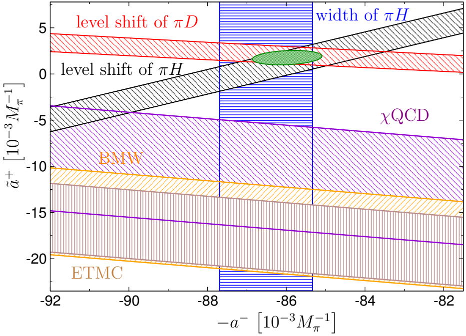

- Inconsistent with the hadronic atom phenomenology

↪ determine the πN scattering lengths on the lattice

Comparison with experimental cross-section data

Unravel the tension around the σ-term comparing with the experimental πN data base

- Generate RS differential cross sections
  - ▷ RS S and P waves
  - ▷ higher partial waves from SAID and KH80 [Workman et al. 2006,2012, Höhler et al. 1980s]
  - ▷ EM interactions implemented using Tromborg proccedure [Tromborg et al. 1977]
- Uncertainties from statistical effects, SL, input variation
  - ▷ below $T_\pi = 50$ MeV uncertainties dominated by scattering length errors
  - $\hookrightarrow$ disentangle RS SL solutions by looking at the data base
- Define:

$$\chi^2_{a^I_{0+}} = \sum_{i,j} \frac{\left(\mathcal{O}^{\text{exp}}{}_{i,j} - \mathcal{O}^{RS}_{i,j}(a^I_{0+})\right)^2}{\Delta\mathcal{O}^{\text{exp}\,2}_{i,j}}$$

- Discrepancy concentrated in the $\pi^+ p \to \pi^+ p$ channel

	RS	KH80
$a^{1/2}_{0+}$ $[10^{-3} M_\pi^{-1}]$	169.8 ± 2.0	173 ± 3
$a^{3/2}_{0+}$ $[10^{-3} M_\pi^{-1}]$	-86.3 ± 1.8	-101 ± 4

Cross-section data: $\pi^+ p \to \pi^+ p$ channel

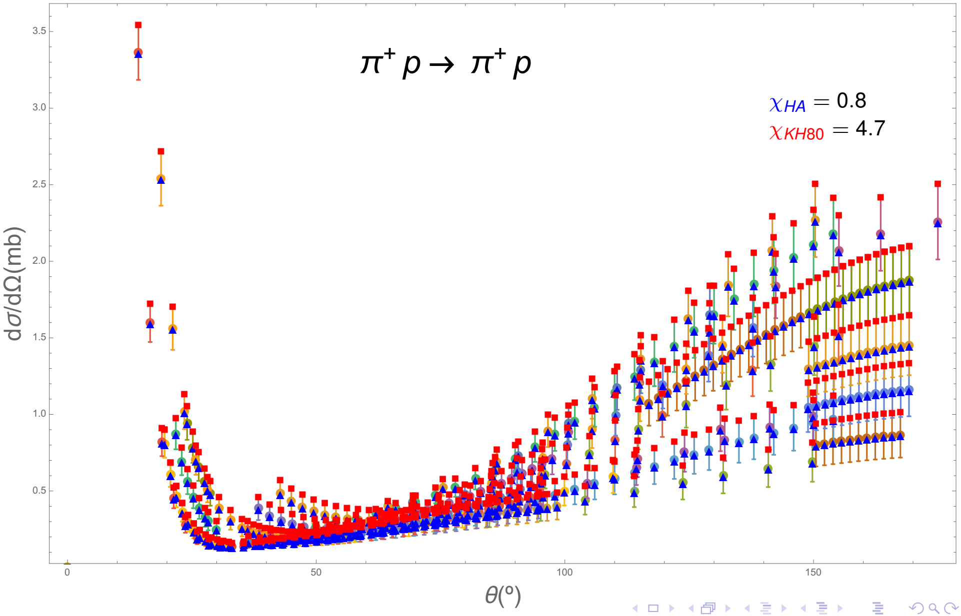

Extracting the σ-term from experimental cross-section data

- Linearized version of RS $d\sigma/d\Omega$ around the HA scattering lengths
- Unbiased fit to the pion-nucleon data base $\Rightarrow$ normalizations constants as fit parameters
- Minimize the χ^2-like as a function of a^I_{0+} and ζ

$$\chi^2(a, a_0, \zeta, \zeta_0, \Delta\zeta_0) = \sum_{k=1}^{N} \chi^2_k(a, a_0, \zeta, \zeta_0, \Delta\zeta_0),$$

$$\chi^2_k(a, a_0, \zeta, \zeta_0, \Delta\zeta_0) = \sum_{i,j=1}^{N_k} \left(\zeta_k^{-1}\sigma(W_i^k, a) - \sigma_i^k\right) \left(C_k^{-1}(a_0, \zeta_0, \Delta\zeta_0)\right)_{ij} \left(\zeta_k^{-1}\sigma(W_j^k, a) - \sigma_j^k\right),$$

$$\left(C_k(a_0, \zeta_0, \Delta\zeta_0)\right)_{ij} = \delta_{ij}\left(\Delta\sigma_i^k\right)^2 + \sigma(W_i^k, a_0)\sigma(W_j^k, a_0)\left(\frac{\Delta\zeta_{0,k}}{\zeta^2_{0,k}}\right)^2, \qquad (1)$$

channel	SL combination	result	HA SL	KH80 SL
$\pi^+ p \to \pi^+ p$	$a_{0+}^{3/2}$	-84.4 ± 1.5	-86.3 ± 1.8	-101 ± 4
$\pi^- p \to \pi^- p$	$(2a_{0+}^{1/2} + a_{0+}^{3/2})/3$	82.5 ± 1.5	84.4 ± 1.7	81.6 ± 2.4
$\pi^- p \to \pi^0 n$	$-\sqrt{2}(a_{0+}^{1/2} - a_{0+}^{3/2})/3$	-122.3 ± 3.4	-120.7 ± 1.3	-129.2 ± 2.4

Nucleon form factor spectral functions

- $\pi\pi \to \bar{N}N$ partial waves + F_π^V pion form factor
  $\hookrightarrow$ $\pi\pi$ contribution to the isovector spectral functions
- Consistent $\pi\pi$ phase shifts in $f_1^\pm$ and F_π^V
  $\hookrightarrow$ Watson theorem is satisfied
- Modern pion form factor data [BaBar 2009, KLOE 2012, BESIII 2015]
- Isospin breaking: $m_p - m_n$ in pole terms, subthreshold parameters, consistent $\rho - \omega$ mixing

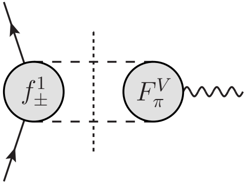

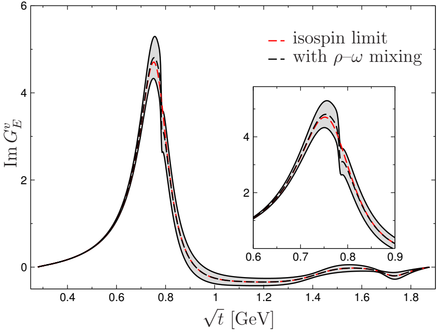

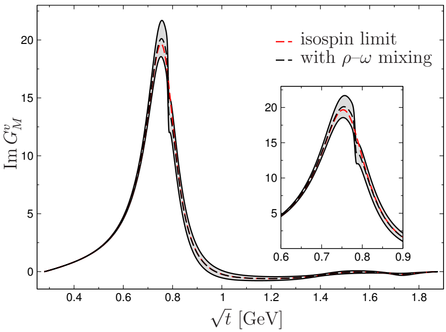

[Hoferichter, Kubis, JRE, Hammer, Meißner 2016]

$\pi\pi$ continuum and proton radius puzzle

- sum rules for the isovector radii: $$\langle r^2_{E/M}\rangle^v = \frac{6}{\pi}\int_{4M_\pi^2}^{\Lambda} dt' \frac{\text{Im}\, G^v_{E/M}(t')}{t'^2}$$

	$\Lambda = 1\,\text{GeV}$	$\Lambda = 2m_N$
$\langle r^2_E\rangle^v\ [\text{fm}^2]$	0.418(32)	0.405(36)
$\langle r^2_M\rangle^v\ [\text{fm}^2]$	1.83(10)	1.81(11)

- correcting normalization by single heavier resonance: ρ', ρ'':
  reduces the radii only to: $\Delta\langle r^2_E\rangle^v = -(0.006\ldots0.008)\,\text{fm}^2$
  $$\Delta\langle r^2_M\rangle^v = -(0.05\ldots0.07)\,\text{fm}^2$$
- with $\langle r^2_E\rangle^n = -0.1161(22)\,\text{fm}^2$ (n scattering on heavy atoms):
  $\hookrightarrow$ proton radius puzzle $\Longleftrightarrow$ isovector radius puzzle

$$\langle r^2_E\rangle^v = 0.412\,\text{fm}^2\ (\mu\text{H}) \quad \text{vs.} \quad \langle r^2_E\rangle^v = 0.442\,\text{fm}^2\ (\text{CODATA})$$

$\triangleright$ mild preference for small proton charge radius [Hoferichter, Kubis, JRE, Hammer, Meißner 2016]

Matching to Chiral Perturbation Theory

Matching to ChPT at the subthreshold point:

- Chiral expansion expected to work best at subthreshold point
  - ▷ maximal distance from threshold singularities
  - ▷ πN amplitude can be expanded as polynomial
- Preferred choice for *NN* scattering due to proximity of relevant kinematic regions

Express the subthreshold parameters in terms of the LECs to $\mathcal{O}(p^4)$

$$d_{00}^{+} = -\frac{2M_\pi^2(2\tilde{c}_1 - \tilde{c}_3)}{F_\pi^2} + \frac{g_a^2(3+8g_a^2)M_\pi^3}{64\pi F_\pi^4} + M_\pi^4\left\{\frac{16\bar{e}_{14}}{F_\pi^2} - \frac{2c_1 - c_3}{16\pi^2 F_\pi^4}\right\}$$

- Chiral πN amplitude to $\mathcal{O}(p^4)$ depends on 13 low-energy constants
- Roy–Steiner system contains 10 subtraction constants
  - ▷ calculate remaining 3 from sum rules
  - ▷ invert the system to solve for LECs

Chiral low-energy constants

	NLO	N^2LO	N^3LO
c_1 [GeV^{-1}]	-0.74 ± 0.02	-1.07 ± 0.02	-1.11 ± 0.03
c_2 [GeV^{-1}]	1.81 ± 0.03	3.20 ± 0.03	3.13 ± 0.03
c_3 [GeV^{-1}]	-3.61 ± 0.05	-5.32 ± 0.05	-5.61 ± 0.06
c_4 [GeV^{-1}]	2.17 ± 0.03	3.56 ± 0.03	4.26 ± 0.04
$\bar{d}_1 + \bar{d}_2$ [GeV^{-2}]	—	1.04 ± 0.06	7.42 ± 0.08
$\bar{d}_3$ [GeV^{-2}]	—	-0.48 ± 0.02	-10.46 ± 0.10
$\bar{d}_5$ [GeV^{-2}]	—	0.14 ± 0.05	0.59 ± 0.05
$\bar{d}_{14} - \bar{d}_{15}$ [GeV^{-2}]	—	-1.90 ± 0.06	-12.18 ± 0.12
$\bar{e}_{14}$ [GeV^{-3}]	—	—	0.89 ± 0.04
$\bar{e}_{15}$ [GeV^{-3}]	—	—	-0.97 ± 0.06
$\bar{e}_{16}$ [GeV^{-3}]	—	—	-2.61 ± 0.03
$\bar{e}_{17}$ [GeV^{-3}]	—	—	0.01 ± 0.06
$\bar{e}_{18}$ [GeV^{-3}]	—	—	-4.20 ± 0.05

- Subthreshold errors tiny, chiral expansion dominates uncertainty
- $\bar{d}_i$ at N^3LO increase by an order of magnitude
  - $\hookrightarrow$ due to terms proportional to $g_A^2(c_3 - c_4) = -16\ \text{GeV}^{-1}$
  - $\hookrightarrow$ mimic loop diagrams with Δ degrees of freedom
- What's going on with chiral convergence?
  - $\hookrightarrow$ look at convergence of threshold parameters with LECs fixed at subthreshold point

Convergence of the chiral series

	NLO	N^2LO	N^3LO	RS
a^+_{0+} $[10^{-3}M_\pi^{-1}]$	-23.8	0.2	-7.9	-0.9 ± 1.4
a^-_{0+} $[10^{-3}M_\pi^{-1}]$	79.4	92.9	59.4	85.4 ± 0.9
a^+_{1+} $[10^{-3}M_\pi^{-3}]$	102.6	121.2	131.8	131.2 ± 1.7
a^-_{1+} $[10^{-3}M_\pi^{-3}]$	-65.2	-75.3	-89.0	-80.3 ± 1.1
a^+_{1-} $[10^{-3}M_\pi^{-3}]$	-45.0	-47.0	-72.7	-50.9 ± 1.9
a^-_{1-} $[10^{-3}M_\pi^{-3}]$	-11.2	-2.8	-22.6	-9.9 ± 1.2
b^+_{0+} $[10^{-3}M_\pi^{-3}]$	-70.4	-23.3	-44.9	-45.0 ± 1.0
b^-_{0+} $[10^{-3}M_\pi^{-3}]$	20.6	23.3	-64.7	4.9 ± 0.8

- N^3LO results bad due to large Delta loops
- matching to ChPT with the explicit Δ's

  $\hookrightarrow$ improvement of the chiral convergence [Siemens, JRE, Epelbaum, Hoferichter, Krebs, Kubis, Meißner 2016]
- Conclusion: lessons for few-nucleon applications

  $\hookrightarrow$ either include the Δ to reduce the size of the loop corrections or use LECs from subthreshold kinematics

  $\hookrightarrow$ error estimates: consider chiral convergence of a given observable, difficult to assign a global chiral error to LECs

The “ruler plot” vs. ChPT

Lattice QCD simulations can be performed at different quark/pion masses

Pion mass dependence of m_N up to NNLO in ChPT, using

- Input from Roy–Steiner solution

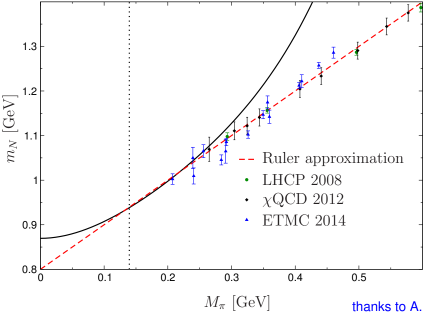

thanks to A. Walker-Loud for providing the lattice data

↪ range of convergence of the chiral expansion is very limited

↪ huge cancellation amongst terms to produce a linear behavior

Roy equations for unphysical pion masses

- Due to the finite domain of validity not solution up to infinity
- Lattice input for each pion mass:

  ▷ high-energy region $s > s_M$

  ▷ high partial waves for all s

  ▷ inelasticities

  ▷ Matching conditions: $\delta_i(s_M)$ and $\delta_i'(s_M)$

  ↪ it seems unlikely the lattice can provide such information, but

- What is the **size** of the **input**?

  ▷ driving terms $Df_J^I \equiv$ all input contribution

  ↪ check their size for different number of subtractions

Subtracted Roy equations for πK scattering

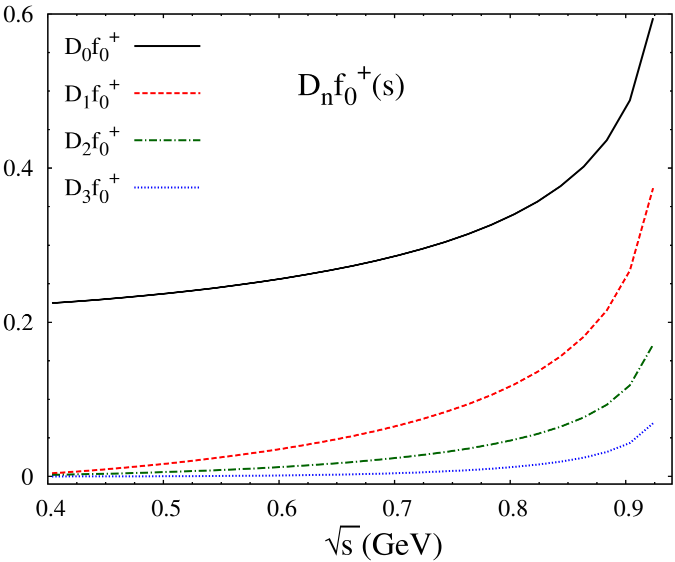

Decomposition of trice subtracted RS for πN

$$\text{Re}\, f^{I_s}_{l\pm}(W) = S^{I_s}_{l\pm}(W) + K_s f(W)^{I_s}_{l\pm} + K_t f(W)^{I_s}_{l\pm} + Df(W)^{I_s}_{l\pm}$$

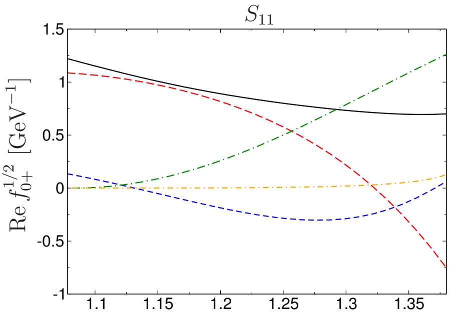

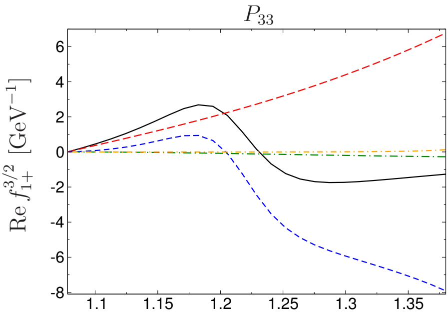

Extrapolation of the solution above s_m

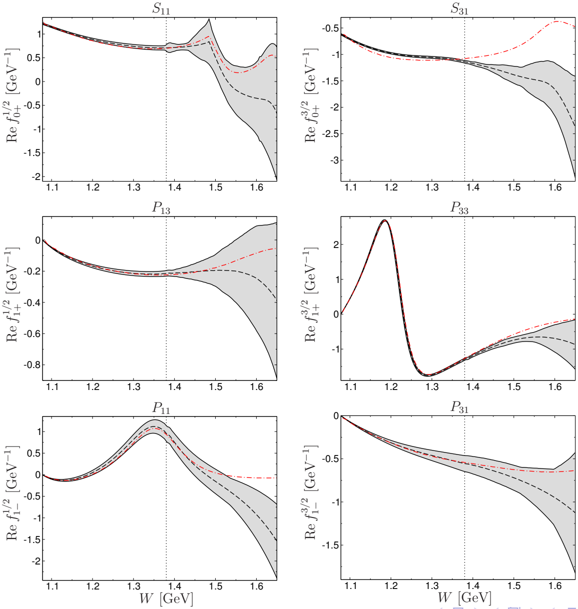

Roy equations for lattice analysis

Conclusions: lesson for lattice results

- **Oversubtracted** Roy equations

  ▷ virtually reduce to zero the dependence on high-energy input

  ↪ driving terms can be included as uncertainties

- Large number of **subtraction constants**

  ▷ uniqueness ⇒ free/fixed number of parameters

  ▷ huge correlations, constraints from sum rules

  ↪ lattice/ChPT input for threshold/subthreshold parameters

- **Extend** the range of validity

  ↪ Roy equations do not break down abruptly above the boundary of their domain of validity

Thank you

Spare slides

Motivation: Why πN scattering?

- **Low energies:** test chiral dynamics in the baryon sector
  $\Rightarrow$ low-energy theorems e.g. for the scattering lengths
- **Higher energies:** resonances, baryon spectrum
- **Input for *NN* scattering:** LECs c_i, πNN coupling

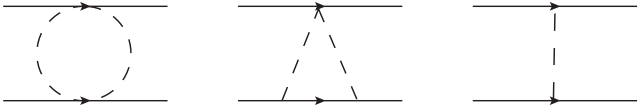

- **Crossed channel $\pi\pi \to \bar{N}N$:** nucleon form factors

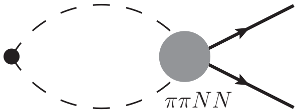

$\Rightarrow$ probe the structure of the nucleon
  - ▷ scalar form factors (S-wave)
  - ▷ electromagnetic form factors (P-waves)
  - ▷ generalized PDF (D-waves)

Phenomenological status

- **Karlsruhe/Helsinki** partial-wave analysis KH80 [Höhler et al. 1980s]

  $\hookrightarrow$ comprehensive analyticity constraints, old data

- Formalism for the extraction of $\sigma_{\pi N}$ via the **Cheng–Dashen low-energy theorem**

  $\hookrightarrow$ “canonical value” $\sigma_{\pi N} \sim 45$ MeV, based on KH80 input [Gasser, Leutwyler, Locher, Sainio 1988,1991]

- **GWU/SAID** partial-wave analysis [Pavan, Strakovsky, Workman, Arndt 2002]

  $\hookrightarrow$ much larger value $\sigma_{\pi N} = (64 \pm 8)$ MeV

- More recently: ChPT in different regularizations (w/ and w/o Δ) [Alarcón et al. 2012]

  $\hookrightarrow$ fit to PWAs, $\sigma_{\pi N} = 59 \pm 7$ MeV

Phenomenological status

- **Karlsruhe/Helsinki** partial-wave analysis KH80 [Höhler et al. 1980s]

  $\hookrightarrow$ comprehensive analyticity constraints, old data

- Formalism for the extraction of $\sigma_{\pi N}$ via the **Cheng–Dashen low-energy theorem**

  $\hookrightarrow$ "canonical value" $\sigma_{\pi N} \sim 45$ MeV, based on KH80 input [Gasser, Leutwyler, Locher, Sainio 1988,1991]

- **GWU/SAID** partial-wave analysis Pavan, Strakovsky, Workman, Arndt 2002

  $\hookrightarrow$ much larger value $\sigma_{\pi N} = (64 \pm 8)$ MeV

- More recently: ChPT in different regularizations (w/ and w/o Δ) [Alarcón et al. 2012]

  $\hookrightarrow$ fit to PWAs, $\sigma_{\pi N} = 59 \pm 7$ MeV

- This talk: two new sources of information on low-energy πN scattering
  - Precision extraction of πN **scattering lengths** from **hadronic atoms** [Baru et al. 2011]
  - **Roy-equation** constraints: analyticity, unitarity, crossing symmetry

Hadronic atoms: constraints for πN

- $\pi H/\pi D$: bound state of π^- and p/d spectrum sensitive to threshold πN amplitude

- Combined analysis of πH and πD:

$$a_0^+ \equiv a^+ = (7.5 \pm 3.1) \cdot 10^{-3} M_\pi^{-1}$$
$$a_0^- \equiv a^- = (86.0 \pm 0.9) \cdot 10^{-3} M_\pi^{-1}$$

  $\hookrightarrow$ Large a^+ suggests a large $\sigma_{\pi N}$,

- But: a^+ very sensitive to isospin breaking, PWA based on $\pi^\pm p$ channels

  $\hookrightarrow$ use instead

$$\frac{a_{\pi^- p} + a_{\pi^+ p}}{2} = (-0.9 \pm 1.4) \cdot 10^{-3} M_\pi^{-1}$$

- Isospin breaking in $\sigma_{\pi N}$ could be important

- We revisit the Cheng-Dashen low-energy theorem

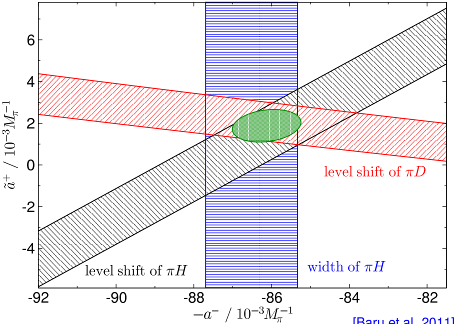

[Baru et al. 2011]

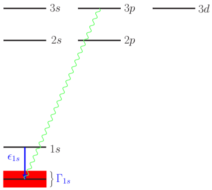

$$\tilde{a}^+ = a^+ + \frac{1}{1 + M_\pi / m_p} \left\{ \frac{M_\pi^2 - m_{\pi^0}^2}{\pi F_\pi^2} c_1 - 2\alpha f_1 \right\}$$

Motivation: Why Roy-Steiner equations?

Roy(-Steiner) eqs. = Partial-Wave (Hyberbolic) Dispersion Relations coupled by unitarity and crossing symmetry

- **Respect all symmetries**: analyticity, unitarity, crossing
- **Model independent** $\Rightarrow$ the actual parametrization of the data is irrelevant once it is used in the integral.
- Framework allows for systematic improvements (subtractions, higher partial waves, ...)
- **PW(H)DRs** help to study processes with high precision:
  - $\pi\pi$-scattering: [Ananthanarayan et al. (2001), García-Martín et al. (2011)]
  - πK-scattering: [Büttiker et al. (2004)]
  - $\gamma\gamma \to \pi\pi$ scattering: [Hoferichter et al. (2011)]

Roy-Steiner equations for πN: flow of information

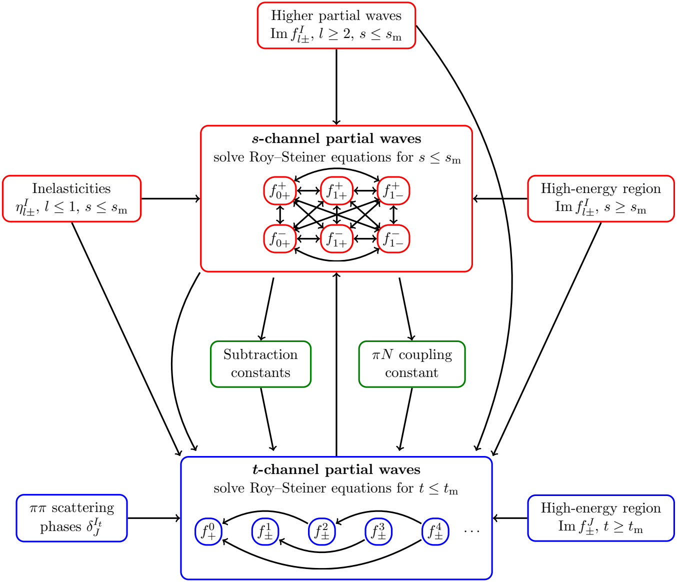

πN-scattering basics

$\pi^a(q) + N(p) \to \pi^b(q') + N(p')$

- **Isospin Structure**:
  $T^{ba} = \delta^{ba} T^+ + \epsilon^{ab} T^-$
- **Lorentz Structure**: $I \in \{+,-\}$
  $T^I = \bar{u}(p') \left(A^I + \frac{\not{q}+\not{q}'}{2} B^I \right) u(p)$
  $D^I = A^I + \nu B^I, \quad \nu = \frac{s-u}{4m}$
- **Isospin basis**: $I_s \in \{1/2, 3/2\}$
  $\{T^+, T^-\} \Leftrightarrow T^{1/2}, T^{3/2}$
- PW projection:
  s-channel pw: $f^I_{l\pm}$
  t-channel pw: $f^J_{\pm}$

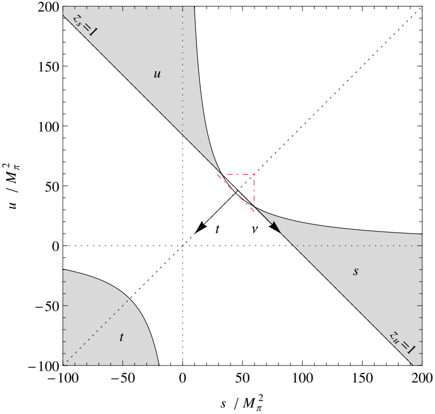

Bose symmetry $\Rightarrow$ even/odd $J \Leftrightarrow I = +/-$

πN-scattering basics: partial waves

- **s-channel** projection:

$$f^I_{l\pm}(W) = \frac{1}{16\pi W}\Big\{(E+m)\left[A^I_l(s)+(W-m)B^I_l(s)\right]+(E-m)\left[-A^I_{l\pm 1}(s)+(W+m)B^I_{l\pm 1}(s)\right]\Big\}$$

$$X^I_l(s) = \int_{-1}^{1} dz_s\, P_l(z_s) X^I(s,t)\Big|_{t=t(s,z_s)=-2q^2(1-z_s)} \quad \text{for } X \in \{A,B\} \text{ and } W=\sqrt{s}$$

- **McDowell symmetry**: $f^I_{l+}(W) = -f^I_{(l+1)-}(-W) \qquad \forall\, l \geq 0$
- **t-channel** projection:

$$f^J_+(t) = -\frac{1}{4\pi}\int_0^1 dz_t\, P_J(z_t)\left\{\frac{p_t^2}{(p_t q_t)^J} A^I(s,t)\Big|_{s=s(t,z_t)} - \frac{m}{(p_t q_t)^{J-1}} z_t B^I(s,t)\Big|_{s=s(t,z_t)}\right\} \qquad \forall\, J \geq 0$$

$$f^J_-(t) = \frac{1}{4\pi}\frac{\sqrt{J(J+1)}}{2J+1}\frac{1}{(p_t q_t)^{J-1}}\int_0^1 dz_t\left[P_{J-1}(z_t) - P_{J+1}(z_t)\right] B^I(s,t)\Big|_{s=s(t,z_t)} \qquad \forall\, J \geq 1$$

- **Bose symmetry** $\Rightarrow$ even/odd $J \Leftrightarrow I = +/-$

πN-scattering basics: Unitarity relations

- **s-channel** unitarity relations ($I_s \in \{1/2, 3/2\}$):

$$\text{Im}\, f_{l\pm}^{I_s}(W) = q\left|f_{l\pm}^{I_s}(W)\right|^2 \theta(W - W_+) + \frac{1 - \left(\eta_{l\pm}^{I_s}(W)\right)^2}{4q}\, \theta(W - W_\text{inel})$$

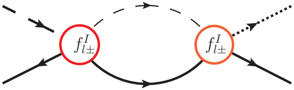

- **t-channel** unitarity relations: 2-body intermediate states: $\pi\pi + \bar{K}K + \cdots$

$$\text{Im}\, f_\pm^J(t) = \sigma_t^\pi \left(t_J^{I_t}(t)\right)^* f_\pm^J(t)\, \theta(t - t_\pi) + 2c_J\sqrt{2}\, k_t^{2J} \sigma_t^K \left(g_J^{I_t}(t)\right)^* h_\pm^J(t)\, \theta(t - t_K)$$

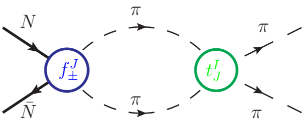

+

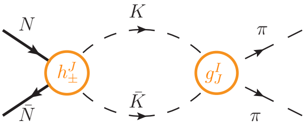

- Only linear in $f_\pm^J(t) \Rightarrow$ less restrictive

Roy-Steiner equations for πN: HDR's

- **Hyperbolic DRs**: $(s-a)(u-a) = b = (s'-a)(u'-a)$ with $a, b \in \mathbb{R}$

$$A^+(s,t;a) = \frac{1}{\pi}\int_{s_+}^{\infty} ds' \left[\frac{1}{s'-s} + \frac{1}{s'-u} - \frac{1}{s'-a}\right] \text{Im}\, A^+(s',t') + \frac{1}{\pi}\int_{t_\pi}^{\infty} dt' \, \frac{\text{Im}\, A^+(s',t')}{t'-t}$$

$$B^+(s,t;a) = N^+(s,t) + \frac{1}{\pi}\int_{s_+}^{\infty} ds' \left[\frac{1}{s'-s} - \frac{1}{s'-u}\right] \text{Im}\, B^+(s',t') + \frac{1}{\pi}\int_{t_\pi}^{\infty} dt' \, \frac{\nu}{\nu'} \frac{\text{Im}\, B^+(s',t')}{t'-t}$$

$$N^+(s,t) = g^2\left(\frac{1}{m^2-s} - \frac{1}{m^2-u}\right)$$

similar for A^-, B^- and N^- [Hite/Steiner (1973)]

- Why **HDR**?
  - Combine all physical regions $\Rightarrow$ crucial for t-channel projection
  - Evade double-spectral regions $\Rightarrow$ the PW decompositions converge
  - Range of convergence can be maximized by tuning the free hyperbola parameter a
  - No kinematical cuts, manageable kernel functions

Roy-Steiner equations for πN: derivation

- Recipe to derive **Roy-Steiner** equations:
  - Expand imaginary parts in terms of s- and t-channel partial waves
  - Project onto s- and t-channel partial waves
  - Combine the resulting equations using s- and t-channel PW unitarity relations
- Similar structure to $\pi\pi$ **Roy equations**
- **Validity**: assuming Mandelstam analyticity
  - s-channel $\Rightarrow$ optimal for $a = -23.2 M_\pi^2$

$$s \in \left[s_+ = (m + M_\pi)^2, 97.30\, M_\pi^2\right] \quad \Leftrightarrow \quad W \in [W_+ = 1.08\ \text{GeV}, 1.38\ \text{GeV}]$$

  - t-channel $\Rightarrow$ optimal for $a = -2.71 M_\pi^2$

$$t \in [t_\pi = 4M_\pi^2, 205.45\, M_\pi^2] \quad \Leftrightarrow \quad \sqrt{t} \in [\sqrt{t_\pi} = 0.28\ \text{GeV}, 2.00\ \text{GeV}]\ .$$

Roy-Steiner equations for πN: subtractions

- **Subtractions** are necessary to ensure the convergence of DR integrals
  $\Rightarrow$ asymptotic behavior

- Can be introduced to lessen the dependence of the low-energy solution on the high-energy behavior

- Parametrize high-energy information in (a priori unknown) subtraction constants
  $\Rightarrow$ matching to ChPT

- Subthreshold expansion around $\nu = t = 0$

$$\bar{A}^+(\nu,t) = \sum_{m,n=0}^{\infty} a_{mn}^+ \nu^{2m} t^n \qquad \bar{B}^+(\nu,t) = \sum_{m,n=0}^{\infty} b_{mn}^+ \nu^{2m+1} t^n \,,$$

$$\bar{A}^-(\nu,t) = \sum_{m,n=0}^{\infty} a_{mn}^- \nu^{2m+1} t^n \qquad \bar{B}^-(\nu,t) = \sum_{m,n=0}^{\infty} b_{mn}^- \nu^{2m} t^n \,,$$

where

$$\bar{A}^+(s,t) = A^+(s,t) - \frac{g^2}{m} \qquad \bar{B}^+(s,t) = B^+(s,t) - g^2\left[\frac{1}{m^2-s} - \frac{1}{m^2-u}\right] \,,$$

$$\bar{A}^-(s,t) = A^-(s,t) \,, \qquad \bar{B}^-(s,t) = B^-(s,t) - g^2\left[\frac{1}{m^2-s} + \frac{1}{m^2-u}\right] + \frac{g^2}{2m^2} \,,$$

- Subthreshold expansion around $\nu = t = 0$

$$A^+(\nu,t) = \frac{g^2}{m} + d^+_{00} + d^+_{01}t + a^+_{10}\nu^2 + \mathcal{O}(\nu^2 t, t^2)$$
$$A^-(\nu,t) = \nu a^-_{00} + a^-_{01}\nu t + a^-_{10}\nu^3 + \mathcal{O}(\nu^5, \nu t^2, \nu^3 t)$$
$$B^+(\nu,t) = g^2 \frac{4m\nu}{(m^2-s_0)^2} + \nu b^+_{00} + \mathcal{O}(\nu^3, \nu t)\ ,$$
$$B^-(\nu,t) = g^2\left[\frac{2}{m^2-s_0} - \frac{t}{(m^2-s_0)^2}\right] - \frac{g^2}{2m^2} + b^-_{00} + b^-_{01}t + +b^-_{10}\nu^2 + \mathcal{O}(\nu^2, \nu^2 t, t^2)$$

- pseudovector Born terms: $D^I = A^I + \nu B^I$

$$\bar{D}^+ = d^+_{00} + d^+_{01}t + d^+_{10}\nu^2$$
$$d^+_{mn} = a^+_{mn} + b^+_{m-1,n}\ , \qquad d^-_{mn} = a^-_{mn} + b^-_{mn}\ .$$

- Sum rules for subthreshold parameters:

$$d^+_{00} = -\frac{g^2}{m} + \frac{1}{\pi}\int_{s_+}^{\infty} \mathrm{d}s'\, h_0(s')\left[\mathrm{Im}\, A^+(s', z'_s)\right]_{(0,0)} + \frac{1}{\pi}\int_{t_\pi}^{\infty}\frac{\mathrm{d}t'}{t'}\left[\mathrm{Im}\, A^+(t', z'_t)\right]_{(0,0)}$$
$$h_0(s') = \frac{2}{s'-s_0} - \frac{1}{s'-a}$$

Solving Roy-Steiner equations for πN: Recoupling schemes

- s-channel subproblem:
  - Kernels are diagonal for $I \in \{+,-\}$, but unitarity relations are diagonal for $I_s \in \{1/2, 3/2\} \Rightarrow$ all partial-waves are interrelated
  - Once the t-channel PWs are known $\Rightarrow$ Structure similar to $\pi\pi$ Roy-equations

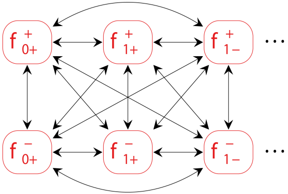

- t-channel subproblem:
  - Only higher PWs couple to lower ones
  - Only PWs with even or odd J are coupled
  - No contribution from f_+^J to f_-^{J+1} $\Rightarrow$ Leads to Muskhelishvili-Omnès problem

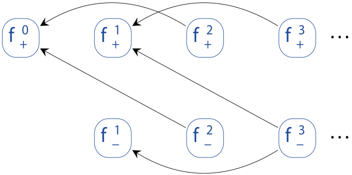

Roy-Steiner equations for πN: s-channel

s-channel RS equations

$$f^I_{l+}(W) = N^I_{l+}(W) + \frac{1}{\pi}\int_{W_+}^{\infty} dW' \sum_{l'=0}^{\infty}\left\{K^I_{ll'}(W,W')\,\mathrm{Im}\, f^I_{l'+}(W') + K^I_{ll'}(W,-W')\,\mathrm{Im}\, f^I_{(l'+1)-}(W')\right\}$$

$$+\frac{1}{\pi}\int_{t_\pi}^{\infty} dt' \sum_J \left\{G_{lJ}(W,t')\,\mathrm{Im}\, f^J_+(t') + H_{lJ}(W,t')\,\mathrm{Im}\, f^J_-(t')\right\}$$

$$= -f^I_{(l+1)-}(-W) \qquad \forall\, l \geq 0\,, \qquad \text{[Hite/Steiner (1973)]}$$

- e $K^I_{ll'}(W,W')$, $G_{lJ}(W,t')$ and $H_{lJ}(W,t')$-Kernels: analytically known,
  e.g. $K^I_{ll'}(W,W') = \frac{\delta_{ll'}}{W'-W} + \ldots \quad \forall\, l, l' \geq 0\,,$
- **Validity**: assuming Mandelstam analyticity
  $\Rightarrow$ optimal for $a = -23.2 M_\pi^2$

$$s \in \left[s_+ = (m+M_\pi)^2, 97.30\, M_\pi^2\right] \quad \Leftrightarrow \quad W \in [W_+ = 1.08\text{ GeV}, 1.38\text{ GeV}]$$

Roy-Steiner equations for πN: t-channel

t-channel RS equations

$$f_+^J(t) = \tilde{N}_+^J(t) + \frac{1}{\pi}\int_{W_+}^{\infty} dW' \sum_{l=0}^{\infty}\Big\{\tilde{G}_{Jl}(t,W')\,\mathrm{Im}\, f_{l+}(W') + \tilde{G}_{Jl}(t,-W')\,\mathrm{Im}\, f_{(l+1)-}(W')\Big\}$$

$$+\frac{1}{\pi}\int_{t_\pi}^{\infty} dt' \sum_{J'}\Big\{\tilde{K}^1_{JJ'}(t,t')\,\mathrm{Im}\, f_+^{J'}(t') + \tilde{K}^2_{JJ'}(t,t')\,\mathrm{Im}\, f_-^{J'}(t')\Big\} \qquad \forall\, J \geq 0\,,$$

$$f_-^J(t) = \tilde{N}_-^J(t) + \frac{1}{\pi}\int_{W_+}^{\infty} dW' \sum_{l=0}^{\infty}\Big\{\tilde{H}_{Jl}(t,W')\,\mathrm{Im}\, f_{l+}(W') + \tilde{H}_{Jl}(t,-W')\,\mathrm{Im}\, f_{(l+1)-}(W')\Big\}$$

$$+\frac{1}{\pi}\int_{t_\pi}^{\infty} dt' \sum_{J'}\tilde{K}^3_{JJ'}(t,t')\,\mathrm{Im}\, f_-^{J'}(t') \qquad \forall\, J \geq 1\,,$$

- **Validity**: assuming Mandelstam analyticity
  $\Rightarrow$ optimal for $a = -2.71 M_\pi^2$

$$t \in [t_\pi = 4M_\pi^2, 205.45\, M_\pi^2] \quad \Leftrightarrow \quad \sqrt{t} \in [\sqrt{t_\pi} = 0.28\ \text{GeV}, 2.00\ \text{GeV}]\,.$$

Solving t-channel: single channel

- Elastic-channel approximation: generic form of the integral equation

$$f(t) = \Delta(t) + (a + bt)(t - 4m^2) + \frac{t^2(t - 4m^2)}{\pi} \int_{t_\pi}^{\infty} dt' \frac{\operatorname{Im} f(t')}{t'(t'^2 - 4m^2)(t' - t)}$$

- $\Delta(t)$: Born terms, s-channel integrals, higher t -channel partial waves $\Rightarrow$ left-hand cut
- Introduce subtractions at $\nu = t = 0 \Rightarrow$ subthreshold parameters a, b
- Solution in terms of Omnès function:

$$\begin{aligned} f(t) =& \Delta(t) + (t - 4m^2)\Omega(t)(1 - t\dot{\Omega}(0))a + t(t - 4m^2)\Omega(t)b \\ &- \Omega(t)\frac{t^2(t - 4m^2)}{\pi}\left\{ \int_{4M_\pi^2}^{t_m} dt' \frac{\Delta(t')\operatorname{Im}\Omega(t')^{-1}}{t'^2(t' - 4m^2)(t' - t)} + \int_{t_m}^{\infty} dt' \frac{\Omega(t')^{-1}\operatorname{Im} f(t')}{t'(t' - 4m^2)(t' - t)} \right\} \end{aligned}$$

$$\Omega(t) = \exp\left\{ \frac{t}{\pi} \int_{t_\pi}^{t_m} \frac{dt'}{t'} \frac{\delta(t')}{t' - t} \right\}$$

Solving t-channel: input and subtractions

- elastic channel approximation: $\sqrt{t_m} = 0.98 - 1.1$ GeV, for $t > t_m$ Im $f^J_\pm(t) = 0$
- First step: check **consistency** with KH80 — Höhler 1983
- Input needed:
  - $\pi\pi$ phase shifts: — Caprini, Colangelo, Leutwyler, (in preparation), Madrid group
  - πN phase shifts: SAID,KH80 — Arndt et al. 2008, Höhler 1983
  - πN at high energies: Regge model — Huang et al. 2010
  - πN parameters: KH80

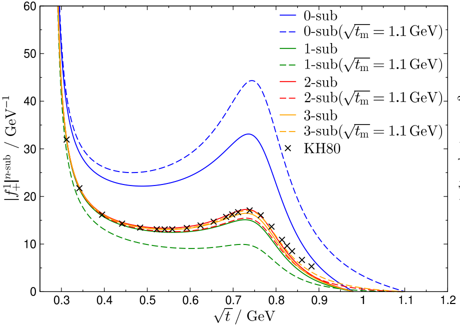

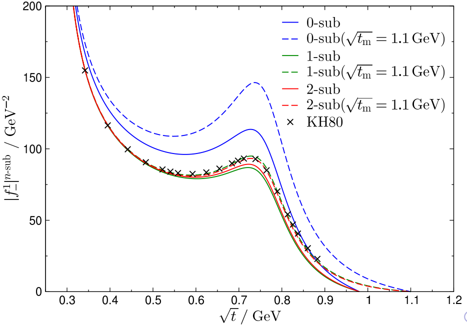

Solving t-channel: P-wave results

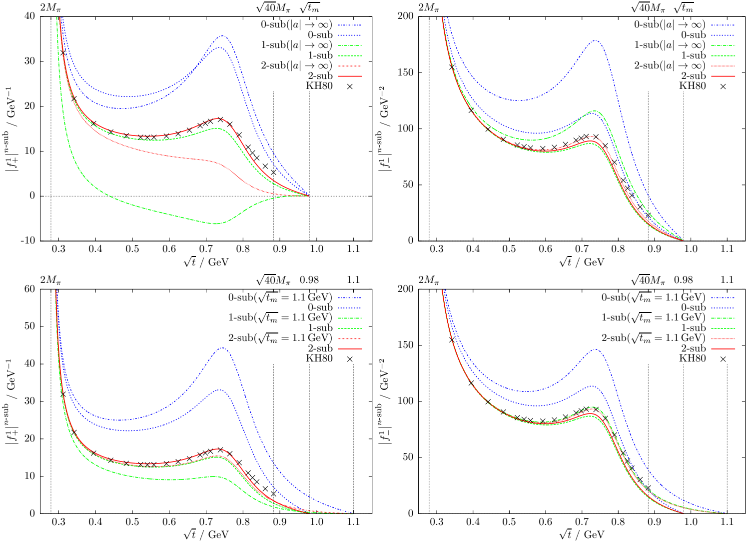

MO solutions in general consistent with KH80 results

Solving t-channel: P, D and F waves up to $\bar{N}N$

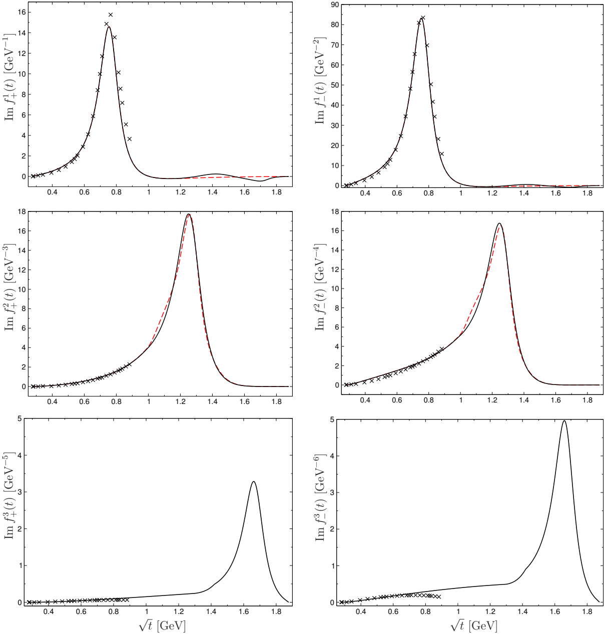

Solving t-channel: coupled channels

- Generic coupled-channel integral equation

$$\mathbf{f}(t) = \mathbf{\Delta}(t) + \frac{1}{\pi}\int_{t_\pi}^{t_m} dt' \frac{T^*(t')\Sigma(t')\mathbf{f}(t')}{t'-t} + \frac{1}{\pi}\int_{t_m}^{\infty} dt' \frac{\operatorname{Im}\mathbf{f}(t')}{t'-t}$$

- Formal solution as in the single-channel case (now with Omnès matrix $\Omega(t)$)

  $\Rightarrow$ Two-channel Muskhelishvili-Omnès problem

$$\mathbf{f}(t) = \begin{pmatrix} f_+^0(t) \\ h_+^0(t) \end{pmatrix} \qquad \operatorname{Im}\Omega(t) = (T(t))^*\Sigma(t)\Omega(t)$$

- Two linearly independent solutions Ω_1, Ω_2 — Muskhelishvili 1953

- In general no analytical solution for the Omnès matrix but for its determinant — Moussallam 2000

$$\det\Omega(t) = \exp\left\{\frac{t}{\pi}\int_{t_\pi}^{t_m} dt' \frac{\psi(t')}{t'(t'-t)}\right\}.$$

Solving t-channel S-wave equations: input

- Input needed:
  - $\pi\pi$ s-wave partial waves: Caprini, Colangelo, Leutwyler, (in preparation)
  - $K\bar{K}$ s-wave partial waves: Büttiker. (2004)
  - πN and KN s-wave pw: SAID, KH80 Arndt et al. 2008, Höhler 1983,
  - πN at high energies: Regge model Huang et al. 2010
  - πN parameters: KH80
  - Hyperon couplings from Jülich model 1989
  - KN subthreshold parameters neglected
- Two-channel approximation beaks down at $\sqrt{t_0} = 1.3$ GeV $\Rightarrow 4\pi$ channel
- From t_0 to $t = 2$ GeV, different approximations considered

Solving t-channel: S-wave results

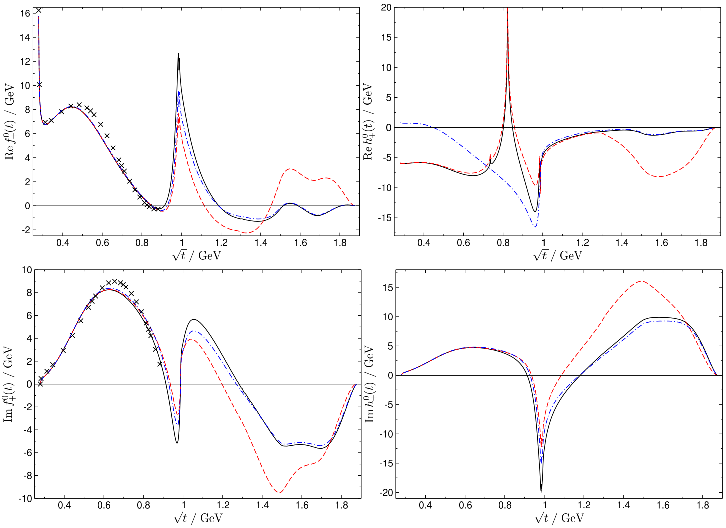

Solving t-channel: S-wave results

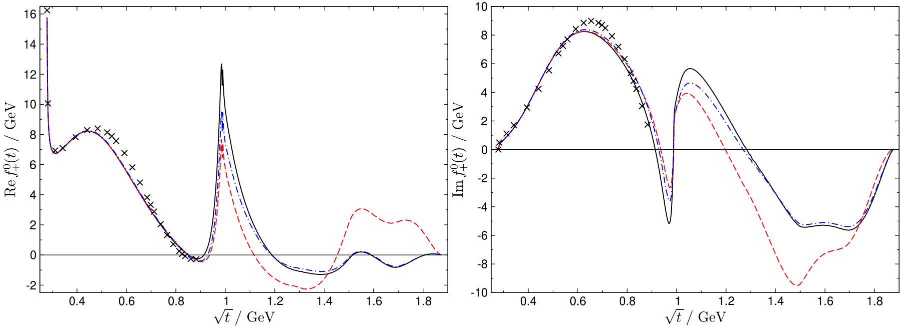

MO solutions in general consistent with KH80 results

Solving s-channel: S-wave results

- General form of the s-channel integral equation

$$f^I_{l+}(W) = \Delta^I_{l+}(W) + \frac{1}{\pi}\int_{W_+}^{\infty} dW' \sum_{l'=0}^{\infty}\left\{K^I_{ll'}(W,W')\,\mathrm{Im}\, f^I_{l'+}(W') + K^I_{ll'}(W,-W')\,\mathrm{Im}\, f^I_{(l'+1)-}(W')\right\}$$

  $\Rightarrow$ form of $\pi\pi$ Roy-Equations
- $\Delta^I_{l+}(W) \equiv$ t-channel contribution and pole term
- valid up to $W_m = 1.38$ GeV
- **Input**:
  - RS t-channel solutions for S and P waves
  - s-channel partial waves for $J > 1$ — SAID analysis
  - s-channel partial waves for $W_m < W < 2.5$ GeV — SAID analysis
  - high energy contribution for $W > 2.5$ GeV: Regge model — Huang et al. 2010
- **Output**:
  - Self-consistent solution for S and P waves for $J \leq J_{\max}$ and $s_{\mathrm{th}} \leq s \leq s_m$
  - Constraints on subtraction constants $\Rightarrow$ subthreshold parameters

Solving s-channel: subtractions

- Existence and uniqueness of solutions — Gasser, Wanders 1999

  $\Rightarrow$ no-cusp condition for each pw + 2 additional constraints are needed

- Take advantage of the precise data for pionic atoms — Gotta et al. 2005, 2010

  $\Rightarrow$ Impose as a **constraint** scattering lengths from a combined analysis of pionic hydrogen and deuterium — Baru et al. 2011

$$a_{0+}^{1/2} = (169.8 \pm 2.0)10^{-3} M_\pi^{-1} \quad a_{0+}^{3/2} = (-86.3 \pm 1.8)10^{-3} M_\pi^{-1}$$

$$\mathrm{Re}\, f_{l\pm}^{I}(s) = \mathbf{q}^{2l} \left(a_{l\pm}^{I} + b_{l\pm}^{I} \mathbf{q}^2 + \cdots \right)$$

10 subthreshold parameters are needed to match **d.o.f**

$\Rightarrow$ **three subtractions**

Solving s-channel: strategy

- Parameterize S and P waves up to $W < W_m$
  - Using SAID partial waves as starting point
- Impose as **constraints** the hadronic atom scattering lengths
- Introduce as many subtractions as necessary to match d.o.f [Gasser, Wanders 1999]
- Minimize difference between LHS and the RHS on a grid of points W_j

$$\chi^2 = \sum_{l,I_s,\pm} \sum_{j=1}^{N} \frac{\left(\mathrm{Re}\, f_{l\pm}^{I_s}(W_j) - F[f_{l\pm}^{I_s}](W_j)\right)^2}{\mathrm{Re}\, f_{l\pm}^{I_s}(W_j)}$$

$F[f_{l\pm}^{I_s}](W_j) \equiv$ right hand side of RS-equations

- Parametrization and subthreshold parameters are the fitting parameters

Solving s-channel: results

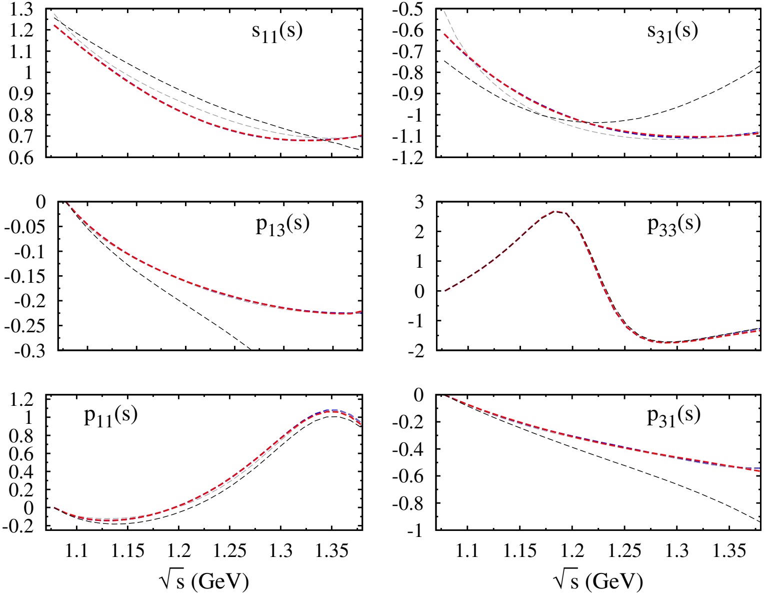

blue/red ⇕ **LHS/RHS** after the fit

gray/black ⇕ **LHS/RHS** before the fit

Notation: $L_{2I_s 2J}$

Results: s-channel PWs

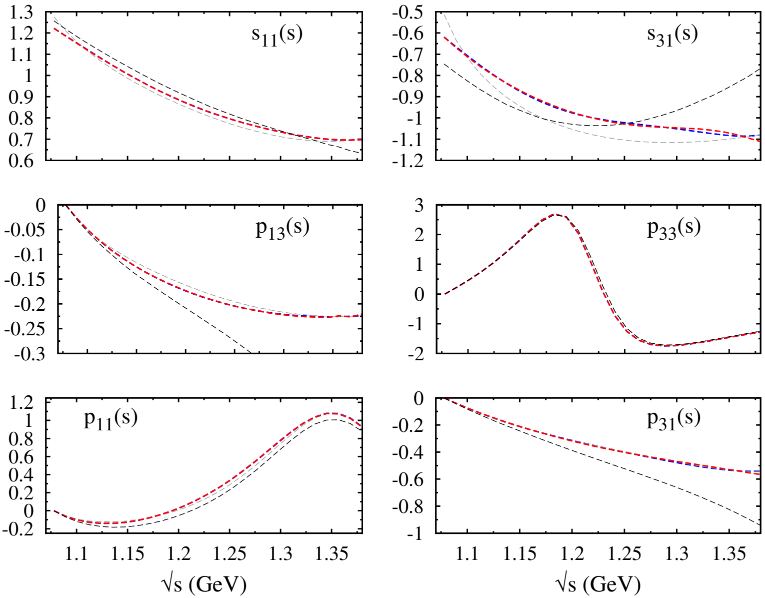

blue/red ⇕ **LHS/RHS**

after the fit

gray/black ⇕ **LHS/RHS**

before the fit

Notation: L_{2I_s2J}

Results: s-channel PWs

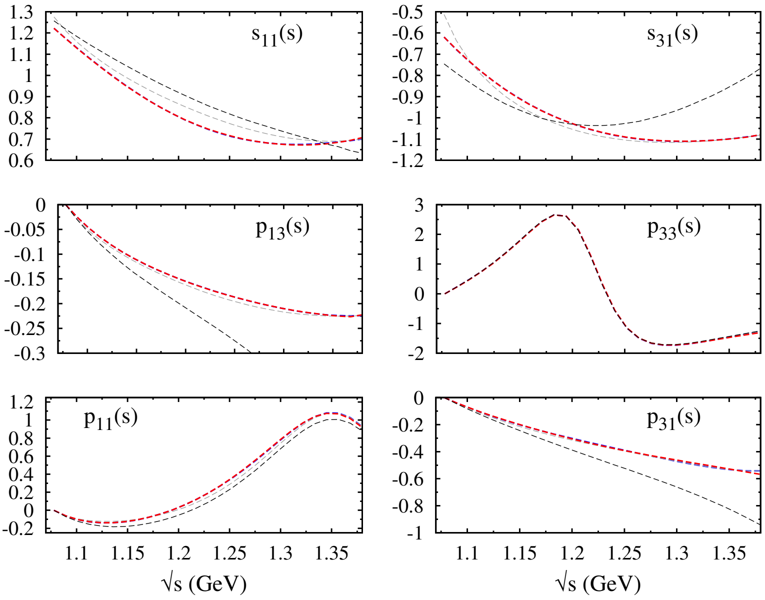

sizable $f_2(1275)$ effect

blue/**re**

⇳

LHS/**RHS**

after the fit

gray/**black**

⇳

LHS/**RHS**

before the fit

Notation: $L_{2I_s 2J}$

Results: t-channel PWs

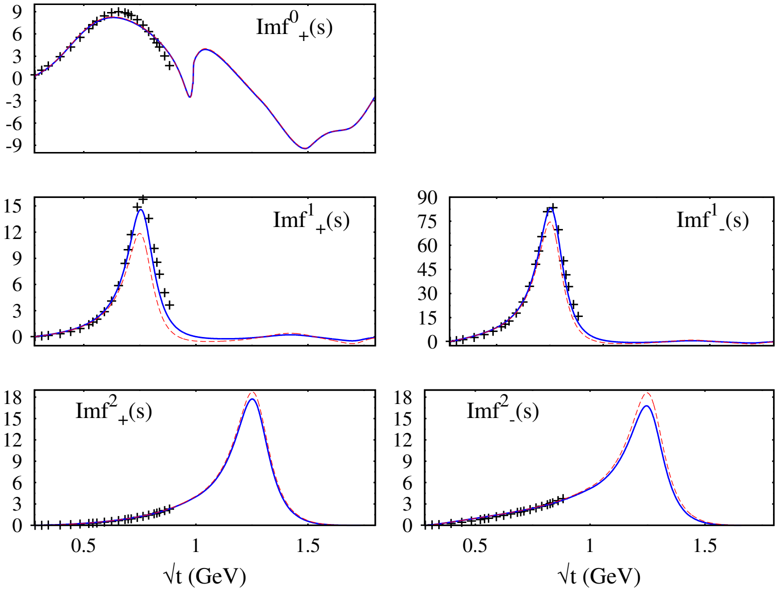

blue
⇕
before the fit
red
⇕
after the fit

+
⇕
KH80

Solving the full RS system: strategy

- Full solution: self-consistent, iterative solution of the full RS system
  ⇒ consistent set of **s**- and **t**-channel PWs & low-energy parameters
- However:
  - t-channel RS eqs. depend only weakly on s-channel PWs
  - resulting s-channel PW change little from **SAID**

A **full solution** can be achieved including in the s-channel RS eqs. the t-channel dependence on the **subthreshold parameters**

Uncertainties

- Statistical errors (at intermediate energies)
  - ▷ important correlations between subthreshold parameters
  - ▷ shallow fit minima
  - ⇒ Sum rules for subthreshold parameters become essential to reduce the errors
- Input variation (small)
  - ▷ small effect for considering s-channel KH80 input
  - ▷ very small effects from $L > 5$ s-channel PWs
  - ▷ small effect from the different S-wave extrapolation for $t > 1.3$ GeV
  - ▷ negligible effect of ρ' and ρ''
  - ▷ very significant effects of the D-waves ($f_2(1275)$)
  - ▷ F-waves shown to be negligible
- matching conditions (close to W_m)
- scattering length (SL) errors (on S-waves and subthreshold parameters)
  - ▷ very important for the $\sigma_{\pi\mathbf{N}}$

Uncertainties: Real part t-channel pw

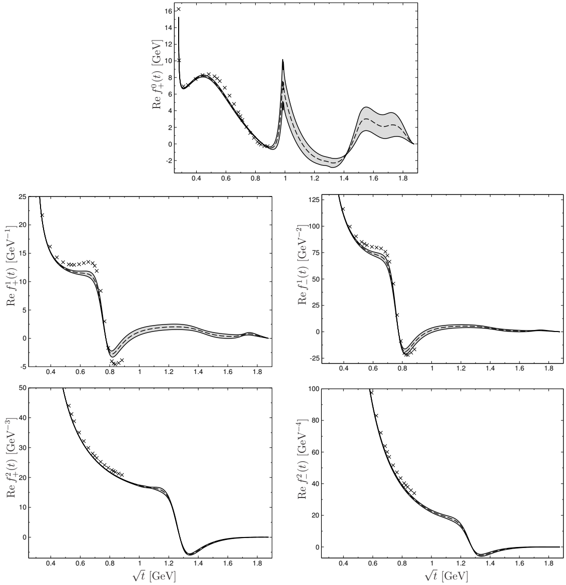

Comparison with KH80

- Karlsruhe-Helsinki analysis **KH80** — Höhler et al. 1980
  - comprehensive analyticity constraints based on fixed-t dispersion relations
  - old experimental data
- Here, an update of **KH80** results with modern input
  - HDR increase the range of validity of the equations
  - πN scattering length extracted from hadronic atoms $\Rightarrow$ essential for the $\sigma_{\pi N}$
  - Goldberger-Miyazawa-Oehme sum rule:

    $g^2_{\pi N}/4\pi = 13.7 \pm 0.2$ — Baru et al. 2011

    compare: $g^2_{\pi N}/4\pi = 14.28$ — Höhler et al. 1983
  - s-channel PWs from **SAID**
  - $f_2(1275)$ included $\Rightarrow$ sizable effect
- **KH80** is internally consistent $\Rightarrow$ RS reproduces **KH80** results with **KH80** input

Results: s-channel PWs with KH80 input

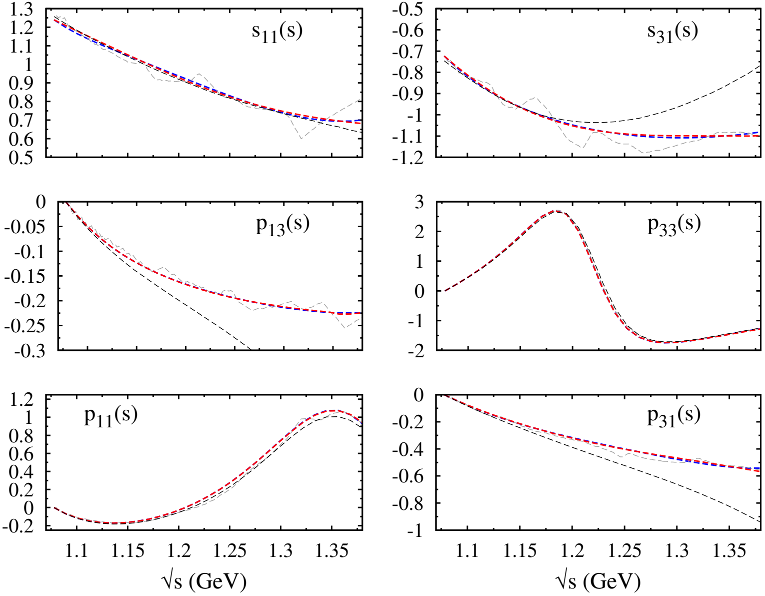

blue/**red**
⇕
LHS/**RHS**
after the fit

gray/**black**
⇕
LHS/**RHS**
before the fit

Notation: $L_{2I_s 2J}$

Results: t-channel PWs with KH80 input

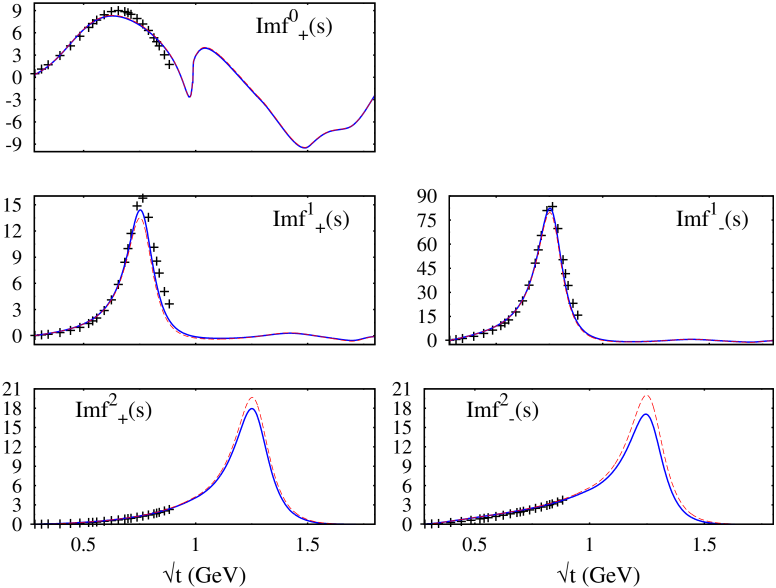

blue

⇕

before the fit

red

⇕

after the fit

+

⇕

KH80

$\sigma_{\pi N}$: comparison with KH80 and SAID

Comparison with KH80

- RS eqs. with KH80 input $\hookrightarrow \sigma_{\pi \mathbf{N}} = 46$ MeV

  $\hookrightarrow$ to be compared with $\sigma_{\pi \mathbf{N}} = 45$ MeV Gasser, Leutwyler, Socher, Sainio 1988, Gasser, Leutwyler, Sainio 1991

  $\hookrightarrow$KH80 is internally **consistent** but at odd with the modern SL determinations

How are d_{00}^+ and d_{01}^+ extracted in KH80 and SAID?

- Standard approach: Gasser, Leutwyler, Locher, Sainio 1988

  replace d_{00}^+ and d_{01}^+ in favor of threshold parameters: a_{0+}^+ and a_{1+}^+

  $\hookrightarrow$ corrections from PWA via DRs (D^+ and E^+)

	Born	a_{0+}^+	a_{1+}^+	D^+	E^+	$\Sigma_d = F_\pi^2 \left(d_{00}^+ + 2M_\pi^2 d_{01}^+\right)$
KH80	-133	-7	**+352**	-91	-72	50
SAID	-127	0	**+351**	-88	-69	67
diff	+6	7	-1	+3	+3	17

- difference with KH80 due the a_{0+}^+
- large weight of a_{1+}^+ $\Rightarrow$ **It has to be known extremely accurately!**

  $\hookrightarrow$ the difference 132.7 (SAID)/131.2 (RS) translates in 5 MeV in the $\sigma_{\pi N}$

Nucleon strangeness

- relate $\sigma_{\pi N}$ to strangeness content of the nucleon:

$$\sigma_{\pi N} = \frac{\hat{m}}{2m_N}\frac{\langle N|\bar{u}u + \bar{d}d - 2\bar{s}s|N\rangle}{1-y} = \frac{\sigma_0}{1-y}, \quad y \equiv \frac{2\langle N|\bar{s}s|N\rangle}{\langle N|\bar{u}u + \bar{d}d|N\rangle}$$

$(m_s - m)\left(\bar{u}u + \bar{d}d - 2\bar{s}s\right) \subset$ LQCD produces SU(3) mass splittings:

$$\sigma_{\pi N} = \frac{\sigma_0}{1-y}, \quad \sigma_0 = \frac{\hat{m}}{m_s - \hat{m}}\left(m_\Xi + m_\Sigma - 2m_N\right) \sim 26\,\text{MeV}$$

higher-order corrections: $\sigma_0 \to (36 \pm 7)$ MeV — Borasoy, Meißner 1997

- potentially large effects
  - ▷ from the decuplet — Alarcon et al. 2013, Siemens et al. 2016
  - ▷ from relativistic corrections (EOMS vs. heavy-baryon)
  - ↪ may increase to $\sigma_0 = (58 \pm 8)$ MeV
- **Conclusion**:
  - ▷ $\sigma_{\pi N} = (59.1 \pm 3.5)$ MeV not incompatible with small y
  - ▷ chiral convergence of σ_0 (hence $\langle N|\bar{s}s|N\rangle$) very doubtful

Threshold parameters

- Threshold parameters defined as: Re $f^I_{l\pm}(s) = q^{2l}\{a^I_{l\pm} + b^I_{l\pm} q^2 + \cdots\}$
- Extracted from hyperbolic sum rules

	RS	KH80
a^+_{0+} $[10^{-3}M_\pi^{-1}]$	-0.9 ± 1.4	-9.7 ± 1.7
a^-_{0+} $[10^{-3}M_\pi^{-1}]$	85.4 ± 0.9	91.3 ± 1.7
a^+_{1+} $[10^{-3}M_\pi^{-3}]$	131.2 ± 1.7	132.7 ± 1.3
a^-_{1+} $[10^{-3}M_\pi^{-3}]$	-80.3 ± 1.1	-81.3 ± 1.0
a^+_{1-} $[10^{-3}M_\pi^{-3}]$	-50.9 ± 1.9	-56.7 ± 1.3
a^-_{1-} $[10^{-3}M_\pi^{-3}]$	-9.9 ± 1.2	-11.7 ± 1.0
b^+_{0+} $[10^{-3}M_\pi^{-3}]$	-45.0 ± 1.0	-44.3 ± 6.7
b^-_{0+} $[10^{-3}M_\pi^{-3}]$	4.9 ± 0.8	13.3 ± 6.0

- Reasonable agreement with KH80 but for the scattering lengths
- Disagreement in the scattering lengths in $\sim 4\sigma$

- Assumption: Mandelstam analyticity — Mandelstam (1958,1959)

  $\Rightarrow$ T(s,t) can be written in terms double spectral densities: ρ_{st}, ρ_{su}, ρ_{ut}

$$T(s,t) = \frac{1}{\pi^2}\iint ds' du' \frac{\rho_{su}(s',u')}{(s'-s)(u'-u)} + \frac{1}{\pi^2}\iint dt' du' \frac{\rho_{tu}(t',u')}{(t'-t)(u'-u)} + \frac{1}{\pi^2}\iint ds' dt' \frac{\rho_{st}(s',t')}{(s'-s)(t'-t)}$$

  $\hookrightarrow$ integration ranges defined by the support of the double spectral densities ρ

- Boundaries of ρ are given lowest lying intermediate states

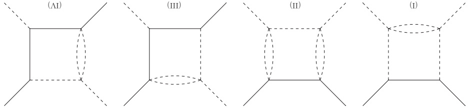

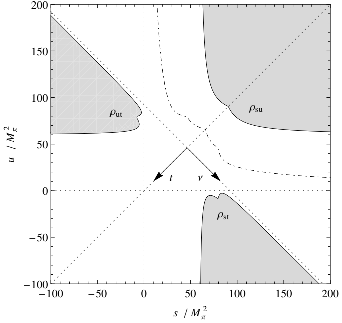

- They limit the range of validity of the HDRS:
  - Pw expansion converge
    $\Rightarrow z = \cos\theta \in$ Lehmann ellipses — Lehmann (1958)
  - the hyperbolae $(s-a)(u-a) = b$ does not enter any double spectral region
    $\Rightarrow$ for a value of a, constraints on b yield ranges in s & t

Dispersion relation for the scalar form factor of the nucleon

- Unitarity relation: $\mathrm{Im}\,\sigma(t) = \frac{2}{4m^2-t}\left\{\frac{3}{4}\sigma_t^\pi \left(F_\pi^S(t)\right)^* f_+^0(t) + \sigma_t^K \left(F_K^S(t)\right)^* h_+^0(t)\right\}$

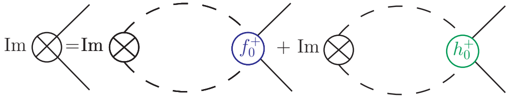

- Once subtracted dispersion relation: $\sigma(t) = \sigma_{\pi N} + \frac{t}{\pi}\int_{t_\pi}^{\infty} dt' \frac{\mathrm{Im}\sigma(t')}{t'(t'-t)}$

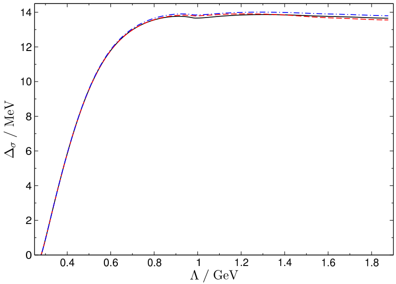

- $\Delta_\sigma = \sigma(2M_\pi^2) - \sigma_{\pi N}$

Dispersion relation for the πN amplitude

- t-channel expansion of the subtracted pseudo-Born amplitude

$$\bar{D}(\nu = 0, t) = 4\pi \left\{ \frac{1}{p_t^2} \bar{f}_0^+(t) + \frac{5}{2} q_t^2 \bar{f}_2^+(t) + \frac{27}{8} p_t^2 q_t^4 \bar{f}_4^+(t) + \frac{56}{16} p_t^4 q_t^6 \bar{f}_6^+(t) + \cdots \right\}$$

- Insert t-channel RS equations for Born-term-subtracted amplitudes $\bar{f}_J^+(t)$

$$\bar{D}(\nu = 0, t) = d_{00}^+ + d_{01}^+ t - 16t^2 \int_{t_\pi}^{\infty} \mathrm{d}t' \frac{\mathrm{Im}\bar{f}_0^+(t')}{t'^2(t' - 4m^2)(t' - t)} + \{J \geq 2\} + \{\text{s-channel integral}\}$$

- $\Delta_D = F_\pi^2 \left(\bar{D}(\nu = 0, t) - d_{00}^+ + d_{01}^+ t\right)$ from evaluation at $t = 2M_\pi^2$

Summary: σ-term corrections

- Nucleon scalar form factor

$$\Delta_\sigma = (13.9 \pm 0.3)\,\text{MeV} + Z_1\left(\frac{g^2}{4\pi} - 14.28\right) + Z_2\left(d_{00}^+ M_\pi + 1.46\right) + Z_3\left(d_{01}^+ M_\pi^3 - 1.14\right) + Z_4\left(b_{00}^+ M_\pi^3 + 3.54\right)$$

$$Z_1 = 0.36\,\text{MeV}\,, \qquad Z_2 = 0.57\,\text{MeV}\,, \qquad Z_3 = 12.0\,\text{MeV}\,, \qquad Z_4 = -0.81\,\text{MeV}$$

- πN amplitude

$$\Delta_D = (12.1 \pm 0.3)\,\text{MeV} + \hat{Z}_1\left(\frac{g^2}{4\pi} - 14.28\right) + \hat{Z}_2\left(d_{00}^+ M_\pi + 1.46\right) + \hat{Z}_3\left(d_{01}^+ M_\pi^3 - 1.14\right) + \hat{Z}_4\left(b_{00}^+ M_\pi^3 + 3.54\right)$$

$$\hat{Z}_1 = 0.42\,\text{MeV}\,, \qquad \hat{Z}_2 = 0.67\,\text{MeV}\,, \qquad \hat{Z}_3 = 12.0\,\text{MeV}\,, \qquad \hat{Z}_4 = -0.77\,\text{MeV}$$

$\hookrightarrow$ most of the dependence on the πN parameters cancels in the difference

Full Correction

$$\Delta_D - \Delta_\sigma = (-1.8 \pm 0.2)\ \text{MeV}$$

Cheng-Dashen theorem in the presence of isospin breaking

- Define as isoscalar as

$$X^+ \to X^p = \frac{1}{2}\left(X_{\pi^+ p \to \pi^+ p} + X_{\pi^- p \to \pi^- p}\right), \qquad X \in \{D, d_{00}, d_{01}, a_{0+} \dots\}$$

  and "isospin limit" by proton and charged pion

- Assume virtual photons to be removed

  $\hookrightarrow$ scenario closest to actual πN PWA

- Calculate IV corrections in SU(2) ChPT, mainly due to $\Delta_\pi = M_\pi^2 - M_{\pi^0}^2$
  - For the σ term no differences at $\mathcal{O}(p^3)$

$$\sigma_{\pi N} = \sigma_p = \sigma_N = -4c_1 M_{\pi^0}^2 - \frac{3g_A^2 M_{\pi^0}^2}{64\pi F_\pi^2}(2M_\pi + M_{\pi^0}) + \mathcal{O}(M_\pi^4)$$

  - Slope of the scalar form factor

$$\Delta_\sigma^p = \sigma_p(2M_\pi^2) - \sigma_p = \frac{3g_A^2 M_\pi^3}{64\pi F_\pi^2} + \frac{g_A^2 M_\pi \Delta_\pi}{128\pi F_\pi^2}\left(-7 + \sqrt{2}\log(3+2\sqrt{2})\right) + \mathcal{O}(M_\pi^4)$$

  - Similarly for Δ_D^p

$$\Delta_D^p = F_\pi^2\left\{\bar{D}_p(0, 2M_\pi^2) - d_{00}^p - 2M_\pi^2 d_{01}^p\right\} = \frac{23g_a^2 M_\pi^3}{384\pi F_\pi^2} + \frac{g_a^2 M_\pi \Delta_\pi}{256\pi F_\pi^2}\left(3 + 4\sqrt{2}\log\left(1+\sqrt{2}\right)\right) + \mathcal{O}(M_\pi^4)$$

- Taking everything together

$$\begin{aligned}\sigma_{\pi N} =& F_\pi^2\left(d_{00}^p + 2M_\pi^2 d_{01}^p\right) - \Delta_R + \Delta_D - \Delta_\sigma + (\Delta_D^p - \Delta_D) - (\Delta_\sigma^p - \Delta_\sigma) \\ &+ \sigma_p(2M_\pi^2) + F_\pi^2 \bar{D}(0, 2M_\pi^2) \\ =& F_\pi^2\left(d_{00}^p + 2M_\pi^2 d_{01}^p\right) - \underbrace{\Delta_R}_{\lesssim 2\text{MeV}} + \underbrace{\Delta_D - \Delta_\sigma}_{(-1.8\pm0.2)\text{MeV}} + \underbrace{\frac{81 g_a^2 M_\pi \Delta_\pi}{256\pi F_\pi^2}}_{3.4\text{MeV}} + \underbrace{\frac{e^2}{2} F_\pi^2 (4f_1 + f_2)}_{(-0.4\pm2.2)\text{MeV}}\end{aligned}$$

↪ sizable corrections from Δ_π increasing the value of the $\sigma_{\pi N}$

$\pi\pi$-continuum contribution to the electromagnetic nucleon form factors

- Electromagnetic nucleon form factor: $\langle N(p')|j^\mu_{\text{em}}|N(p)\rangle = \bar{u}(p')\left[F_1^N(t)\gamma^\mu + \frac{i\sigma^{\mu\nu}q_\nu}{2m_N}F_2^N(t)\right]u(p),$

$$G_E^N(t) = F_1^N(t) + \frac{t}{4m_N^2}F_2^N(t), \quad G_M^N(t) = F_1^N(t) + F_2^N(t).$$

- first inelastic correction from $\pi\pi$ continuum

$$\text{Im}\, G_E^v(t) = \frac{q_t^3}{m_N\sqrt{t}}\left(F_\pi^V(t)\right)^* f_+^1(t)\theta(t-t_\pi)$$
$$\text{Im}\, G_M^v(t) = \frac{q_t^3}{\sqrt{2t}}\left(F_\pi^V(t)\right)^* f_-^1(t)\theta(t-t_\pi)$$

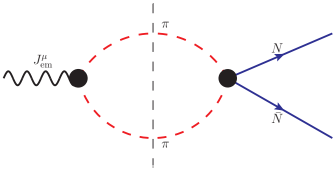

$\hookrightarrow$ rigorous constraint fixed from:

- ▷ RS t-channel partial waves
- ▷ pion form factor

- update of Höhler spectral functions, including also isospin breaking

criticism by Lee et al. 2015

$\pi\pi$-continuum: $\rho - \omega$ mixing

- Isovector and isoscalar nucleon form factor

$$F_i^s(t) = \frac{1}{2}\left(F_i^p(t) + F_i^n(t)\right), \quad F_i^v(t) = \frac{1}{2}\left(F_i^p(t) - F_i^n(t)\right)$$

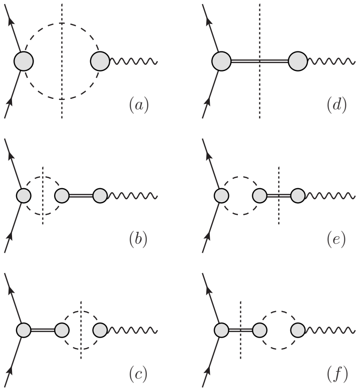

$$\begin{aligned}
\mathrm{Im}\, G_E^v(t) &= \frac{q_t^3}{m_N\sqrt{t}} |\Omega_1^1(t)||f_+^1(t)|\theta(t-t_\pi) \\
&\times \left(1 + \alpha t + \frac{\varepsilon\, t}{M_\omega^2 + iM_\omega\Gamma_\omega - t}\right) \\
&+ \varepsilon\, \mathrm{Im}\left(\frac{t}{M_\omega^2 - iM_\omega\Gamma_\omega - t}\right) \\
&\times \frac{1}{\pi}\int_{t_\pi}^{\infty} \mathrm{d}t' \frac{\frac{q_t'^3}{m_N\sqrt{t'}}|\Omega_1^1(t')||f_+^1(t')|}{t' - t - i\varepsilon}, \\
\mathrm{Im}\, G_M^v(t) &= \frac{q_t^3}{\sqrt{2t}} |\Omega_1^1(t)||f_-^1(t)|\theta(t-t_\pi) \\
&\times \left(1 + \alpha t + \frac{\varepsilon\, t}{M_\omega^2 + iM_\omega\Gamma_\omega - t}\right) \\
&+ \varepsilon\, \mathrm{Im}\left(\frac{t}{M_\omega^2 - iM_\omega\Gamma_\omega - t}\right) \\
&\times \frac{1}{\pi}\int_{t_\pi}^{\infty} \mathrm{d}t' \frac{\frac{q_t'^3}{\sqrt{2t'}}|\Omega_1^1(t')||f_-^1(t')|}{t' - t - i\varepsilon}.
\end{aligned}$$

Chiral Low Energy Constants with Δ's

	HB-NN		HB-πN		covariant	
N^{2}LO	Q^3	ϵ^3	Q^3	ϵ^3	Q^3	ϵ^3
c_1	−1.08(2)	−1.25(3)	−1.08(2)	−1.24(3)	−1.00(2)	−1.19(4)
c_2	3.26(3)	1.71(1.01)	3.26(3)	1.13(1.02)	2.55(3)	1.14(19)
c_3	−5.39(5)	−2.68(84)	−5.39(5)	−2.75(84)	−4.90(5)	−2.56(40)
c_4	3.62(3)	1.57(16)	3.62(3)	1.58(16)	3.08(3)	1.33(20)
d_{1+2}	1.02(6)	0.14(17)	1.02(6)	−0.07(18)	1.78(6)	0.62(16)
d_3	−0.46(2)	−0.84(14)	−0.46(2)	−0.48(15)	−1.12(2)	−1.45(5)
d_5	0.15(5)	0.80(7)	0.15(5)	0.47(6)	−0.05(5)	0.29(6)
d_{14-15}	−1.85(6)	−1.09(30)	−1.85(6)	−0.72(31)	−2.27(6)	−0.98(13)
N^{3}LO	Q^4	ϵ^4	Q^4	ϵ^4	Q^4	ϵ^4
c_1	−1.11(3)	−1.11(3)	−1.11(3)	−1.11(3)	−1.12(3)	−1.10(3)
c_2	3.61(4)	1.41(38)	3.17(3)	1.28(20)	3.35(3)	1.16(20)
c_3	−5.60(6)	−1.88(45)	−5.67(6)	−2.04(39)	−5.70(6)	−2.10(39)
c_4	4.26(4)	2.03(28)	4.35(4)	2.07(29)	3.97(3)	1.91(27)
d_{1+2}	6.37(9)	1.78(31)	7.66(9)	2.90(30)	4.70(7)	1.78(24)
d_3	−9.18(9)	−3.64(36)	−10.77(10)	−5.91(50)	−5.26(5)	−3.25(14)
d_5	0.87(5)	1.52(7)	0.59(5)	1.03(7)	0.31(5)	0.66(6)
d_{14-15}	−12.56(12)	−4.38(54)	−13.44(12)	−5.17(55)	−8.84(10)	−3.41(41)
e_{14}	1.16(4)	1.64(10)	0.85(4)	1.12(16)	1.17(4)	1.28(11)
e_{15}	−2.26(6)	−4.95(15)	−0.83(6)	−3.30(25)	−2.58(7)	−3.07(13)
e_{16}	−0.29(3)	4.21(16)	−2.75(3)	1.92(43)	−1.77(3)	1.71(17)
e_{17}	−0.17(6)	−0.44(6)	0.03(6)	−0.39(7)	−0.45(6)	−0.51(7)
e_{18}	−3.47(5)	1.34(29)	−4.48(5)	0.67(31)	−1.68(5)	1.30(17)

Threshold kinematics from subthreshold with Δ's

	HB-NN		HB-πN		covariant		RS
N^{2}LO	Q^3	ϵ^3	Q^3	ϵ^3	Q^3	ϵ^3	
a^+_{0+} $[10^{-3}M_\pi^{-1}]$	0.5	−9.8(10.9)	0.5	−0.4(9.2)	−14.8	1.0(17.3)	−0.9(1.4)
a^-_{0+} $[10^{-3}M_\pi^{-1}]$	92.2	92.7(1.0)	92.9	90.5(9)	89.9	81.7(1.6)	85.4(9)
a^+_{1+} $[10^{-3}M_\pi^{-3}]$	113.8	125.8(16.7)	121.7	127.2(18.4)	116.4	128.5(9.6)	131.2(1.7)
a^-_{1+} $[10^{-3}M_\pi^{-3}]$	−74.8	−77.4(2.5)	−75.5	−78.4(2.6)	−75.1	−79.7(3.0)	−80.3(1.1)
a^+_{1-} $[10^{-3}M_\pi^{-3}]$	−54.1	−53.4(14.1)	−47.0	−52.5(15.8)	−55.5	−52.5(8.5)	−50.9(1.9)
a^-_{1-} $[10^{-3}M_\pi^{-3}]$	−14.1	−13.1(2.7)	−2.5	−7.8(3.0)	−10.4	−9.7(4.1)	−9.9(1.2)
b^+_{0+} $[10^{-3}M_\pi^{-3}]$	−45.7	−38.1(9.6)	−22.1	−23.7(14.4)	−50.9	−34.7(12.1)	−45.0(1.0)
b^-_{0+} $[10^{-3}M_\pi^{-3}]$	35.9	26.4(1.0)	22.6	17.6(8)	21.6	14.2(2.0)	4.9(8)
N^{3}LO	Q^4	ϵ^4	Q^4	ϵ^4	Q^4	ϵ^4	
a^+_{0+} $[10^{-3}M_\pi^{-1}]$	−1.5	−1.5(8.5)	−8.0	1.2(20.4)	−5.7	−0.8(10.3)	−0.9(1.4)
a^-_{0+} $[10^{-3}M_\pi^{-1}]$	68.5	96.3(2.0)	58.6	70.0(3.3)	83.8	83.6(1.9)	85.4(9)
a^+_{1+} $[10^{-3}M_\pi^{-3}]$	134.3	136.0(9.7)	132.1	135.2(8.7)	128.0	132.7(9.0)	131.2(1.7)
a^-_{1+} $[10^{-3}M_\pi^{-3}]$	−80.9	−80.0(3.4)	−90.1	−86.4(2.7)	−78.1	−81.1(3.6)	−80.3(1.1)
a^+_{1-} $[10^{-3}M_\pi^{-3}]$	−55.7	−47.5(10.5)	−73.7	−56.9(7.1)	−53.5	−51.4(7.9)	−50.9(1.9)
a^-_{1-} $[10^{-3}M_\pi^{-3}]$	−10.0	−5.6(4.9)	−23.7	−14.4(6.5)	−11.8	−10.4(5.7)	−9.9(1.2)
b^+_{0+} $[10^{-3}M_\pi^{-3}]$	−42.2	−31.4(8.1)	−44.5	−32.6(21.3)	−54.7	−33.9(8.5)	−45.0(1.0)
b^-_{0+} $[10^{-3}M_\pi^{-3}]$	−31.6	7.1(2.3)	−65.2	−34.1(5.7)	2.3	2.9(2.1)	4.9(8)

Goldberger-Miyazawa-Oehme sum rule

- Fixed-t dispersion relations at threshold $\hookrightarrow$ **GMO sum rule**

$$\frac{g^2}{4\pi} = \left(\left(\frac{m_p + m_n}{M_\pi}\right)^2 - 1\right)\left\{\left(1 + \frac{M_\pi}{m_p}\right)\frac{M_\pi}{4}\left(a_{\pi^- p} - a_{\pi^+ p}\right) - \frac{M_\pi^2}{2} J^-\right\}$$

$$= 13.69 \pm 0.12 \pm 0.15$$

$$J^- = \frac{1}{4\pi^2}\int_0^\infty dk \frac{\sigma^{\text{tot}}_{\pi^- p}(k) - \sigma^{\text{tot}}_{\pi^+ p}(k)}{\sqrt{M_\pi^2 + k^2}}$$

- J^- known very accurately

Ericson et al. 2002, Abaev et al. 2007

- other determinations

	de Swart et al. 97	Arndt et al. 94	Ericson et al. 02	Bugg et al. 73	KH80
method	NN	πN	GM0	πN	πN
$g^2/4\pi$	13.54 ± 0.05	13.75 ± 0.15	14.11 ± 0.20	14.30 ± 0.18	14.28

- With KH80 scattering lengths $g^2/4\pi = 14.28$ is reproduced exactly

$\hookrightarrow$ discrepancy related to old scattering length values

Spin-independent WIMP–nucleon scattering

- Effective Lagrangian

$$\mathcal{L} = C_{qq}^{SS} \frac{m_q}{\Lambda^3} \bar{\chi}\chi \, \bar{q}q + C_{qq}^{VV} \frac{m_q}{\Lambda^2} \bar{\chi}\gamma^\mu\chi \, \bar{q}\gamma_\mu q + \bar{C}_{gg}^{S} \frac{\alpha_S}{\Lambda^3} \bar{\chi}\chi G_{\mu\nu} G^{\mu\nu}$$

- WIMP χ **Dirac fermion** and **SM singlet**
- Spin–independent cross section at vanishing momentum transfer

$$\sigma_N^{SI} = \frac{\mu_\chi^2}{\Lambda^4} \left| \left(\frac{m_N}{\Lambda} C_{qq}^{SS} f_q^N - 12\pi C_{gg}^{S} f_Q^N \right) + C_{qq}^{VV} f_V^N \right|^2$$

$$\mu_\chi = \frac{m_\chi m_N}{m_\chi + m_N} \quad f_q^N = 2 \quad f_q^N = \frac{\sigma_{\pi \mathbf{N}}(1-\xi)}{m_N} + \Delta f_q^N$$

- nucleon-matrix elements dominated by $\sigma_{\pi \mathbf{N}}$

Dispersion relations: unitarity

- unitarity ⇒ conservation of probability $SS^\dagger = S^\dagger S = \mathbb{I}$

$$\mathrm{Im}t_{IJ} = \sum_n \sigma_n(s) t_{IJ}(s)^n t_{IJ}(s)^{n\,*} \Rightarrow \qquad t_{IJ}^{f\,i}(s) = \frac{\eta_{IJ}^{f\,i}(s) e^{2i\delta_{IJ}^{f\,i}(s)} - 1}{2i\sigma(s)}$$

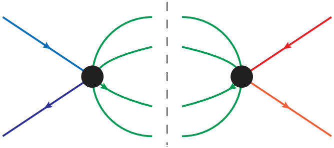

- $\mathrm{Im}t_{IJ} \neq 0$ above the first production threshold ⇒ Right-Hand-Cut (RHC)
- for elastic scattering

$$\mathrm{Im}t_{IJ}(s) = \sigma(s)|t_{IJ}(s)|^2 \Rightarrow \mathrm{Im}t_{IJ}^{-1}(s) = -\sigma(s), \qquad \sigma(s) = \sqrt{1 - \frac{4m^2}{s}}$$

- $\mathrm{Im}t_{IJ}$ on the physical region known exactly
- Unitarization methods ⇒ estimate $\mathrm{Re}t_{IJ}$

Dispersion relations: crossing symmetry

- Mandelstam hypothesis:
  $\hookrightarrow$ analytical continuation of T(s,t,u)

$$T(s,t,u) = \begin{cases} T_{12\to34}(s,t,u), & s \geq 4m^2, \quad t \leq 0, \quad u \leq 0, \\ T_{1\bar{3}\to\bar{2}4}(t,s,u), & t \geq 4m^2, \quad s \leq 0, \quad u \leq 0, \\ T_{1\bar{4}\to3\bar{2}}(u,t,s), & u \geq 4m^2, \quad s \leq 0, \quad t \leq 0, \end{cases}$$

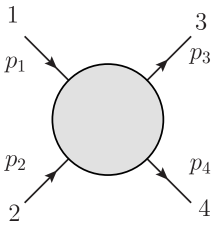

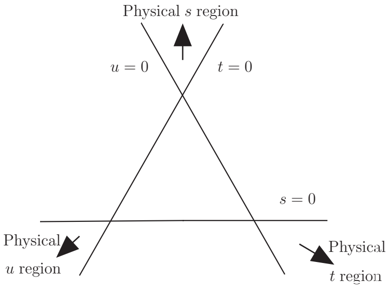

- Assumption for the analytical structure of T needed
  $\hookrightarrow$ dynamical origin of the singularities

Dispersion relations: analyticity

- Singularities have a dynamical origin
  - poles on the real axis

    ↪ bound states
  - poles on the the complex plane forbidden by causality

    ↪ resonances are poles on higher Riemann sheets
  - physical thresholds

    $$T(s+i\epsilon,t,u) - T(s-i\epsilon,t,u) = T(s+i\epsilon,t,u) - T(s+i\epsilon,t,u)^* = 2i\mathrm{Im}T(s,t,u)$$

    Schwartz reflection principle: $T(s^*,t,u) = T(s,t,u)^*$
  - Unitarity imposes $\mathrm{Im}T(s,t,u) \neq 0$ for $s > 0$ and $s < t$

    ↪ cuts ⇒ RHC and LHC

Summary

- Derived a closed system of Roy–Steiner equations for πN
- Numerical solution and error analysis of the full system of RS eqs.
- Precise determination of the $\sigma_{\pi N}$
  - ▷ Roy–Steiner formalism reproduces KH80 result with KH80 input
  - ▷ With modern input for scattering lengths and coupling constant $\sigma_{\pi N}$ increases
  - ▷ results from hadronic atom results compatible with low-energy πN scattering data
- t- channel $\rightarrow$ nucleon form factor spectral functions

  sum rules for isovector radii $\rightarrow$ proton radius puzzle
- Extraction of the ChPT LECs
- Study of the chiral convergence